Deliverable D32 (D4.11)

Initial Analysis of the hot spot pilot results

RI-URBANS

Research Infrastructures Services Reinforcing Air Quality Monitoring Capacities in European Urban & Industrial AreaS (GA n. 101036245)

By

KNMI, INOE, ISAC, JRC, TU-Delft, TNO & UHEL

26th March 2024

RI-URBANS (http://www.RIURBANS.eu) is supported by the European Commission under the Horizon 2020 – Research and Innovation Framework Programme, H2020-GD-2020, Grant Agreement number: 101036245

Deliverable D32 (D4.11): Initial analysis of the hot spot pilot results

Authors: Arnoud Apituley (KNMI), Diego Alves Gouveia (KNMI), Mirjam den Hoed (KNMI), Steven Knoop (KNMI), Marijn de Haij (KNMI), Doina Nicolae (INOE), Camilla Perfetti (ISAC-CNR), Laura Renzi (ISAC-CNR), Nora Zannoni (ISAC-CNR), Valeria Paola Mardonez Balderrama (ISAC-CNR), Cecilia Magnani (ISAC-CNR), Ferdinando Pasqualini (ISAC-CNR), Luca Di Liberto (ISAC-CNR), Francesca Barnaba (ISAC-CNR), Angela Marinoni (ISAC-CNR), Cristina Colombi (ARPA Lombardia), Jean Philippe Putaud (JRC), Fabrizia Cavalli (JRC), Bart Speet (TNO), Arjan Hensen (TNO), Stephan de Roode (TU-Delft), Myriam Argo (UHEL) & Federico Bianchi (UHEL)

Work package (WP)	WP4 - Pilot implementations for testing and demonstrating services
Deliverable	D32 (D4.11)
Lead beneficiary	KNMI
Deliverable type	■ R (document, report) ☐ DEC (websites, patent filings, videos,….) ☐ Other: ORDP (open research data pilot)
Dissemination level	■ PU (public) ☐ CO (confidential, only members of consortium and European Commission))
Estimated delivery deadline	M30 (31/03/2024)
Actual delivery deadline	26/03/2024
Version	Final
Reviewed by	WP4 leaders and the project coordinators
Accepted by	Project coordination team
Comments	This report describes measurement campaigns initiated for the pilots on hotspots and mapping of pollutants in Rotterdam-Amsterdam, Bucharest, and Milano-Bologna (T4.5).

RI-URBANS (http://www.RIURBANS.eu) is supported by the European Commission under the Horizon 2020 – Research and Innovation Framework Programme, H2020-GD-2020, Grant Agreement number: 101036245

Table of Contents

RI-URBANS (http://www.RIURBANS.eu) is supported by the European Commission under the Horizon 2020 – Research and Innovation Framework Programme, H2020-GD-2020, Grant Agreement number: 101036245

1. About this document

The WP4 tackles OJB4 to test and to demonstrate solutions for advanced urban air quality (AQ) monitoring systems and evaluation of exposures, which are proposed by WP1-3, at representative areas and hot spots in Europe. Specifically, it will implement 5 testing and demonstration pilots in 9 European cities (Athens, Barcelona, Birmingham, Bucharest, Helsinki, Milano, Paris, Rotterdam-Amsterdam and Zurich, with at least 3 cities in each pilot). In the scope of WP4, the task T4.5 focuses on mapping and characterizing hotspots for pollution emissions and concentrations in urban areas with intensive traffic and/or industrial activities, aiding in the evaluation of pollutant exposure and policy-making. To accomplish that, the pilot cities of Rotterdam-Amsterdam (The Netherlands), Bucharest (Romania) and Milano-Bologna (Italy) were selected as representative European areas for intensive measurement campaigns.

This deliverable D32 (D4.11) reports on initial analysis of the pilot measurement campaigns for hotspots in the selected cities, as previously described in milestone M27 (M4.11).

This is a public document, available in the RI-URBANS website (https://riurbans.eu/work-package-4/#milestones-wp4). The document will be distributed to all RI-URBANS partners for their use and submitted to European Commission as the RI-URBANS Deliverable D32 (D4.11).

2. Initial Analysis of the Hot-Spot pilot results

This chapter gives a short summary of the observational campaigns that were initiated in the selected pilot cities, as a follow up for the plans described previously in the milestone M4.10. It is worth mentioning that many of the measurement campaign efforts have strong connections (but not limited) to tasks that focuses on the urban mapping (T4.3 and T2.3).

2.1 Rotterdam campaign

2.1.1 Rotterdam

The city of Rotterdam is characterised by its harbour and associated industrial activities. The city is located at the estuary of the river Maas and therefore also closely connected to the North Sea (Figure 2.1.1). The residential aera (population roughly 1 million residents) is situated further inland, while the harbour and industry are stretched out along the river and the 'Nieuwe Waterweg' canal. In the industrial area there are various hot spots of air pollution. In particular the petrochemical industry and a coal fire power plant.

RI-URBANS (http://www.RIURBANS.eu) is supported by the European Commission under the Horizon 2020 – Research and Innovation Framework Programme, H2020-GD-2020, Grant Agreement number: 101036245

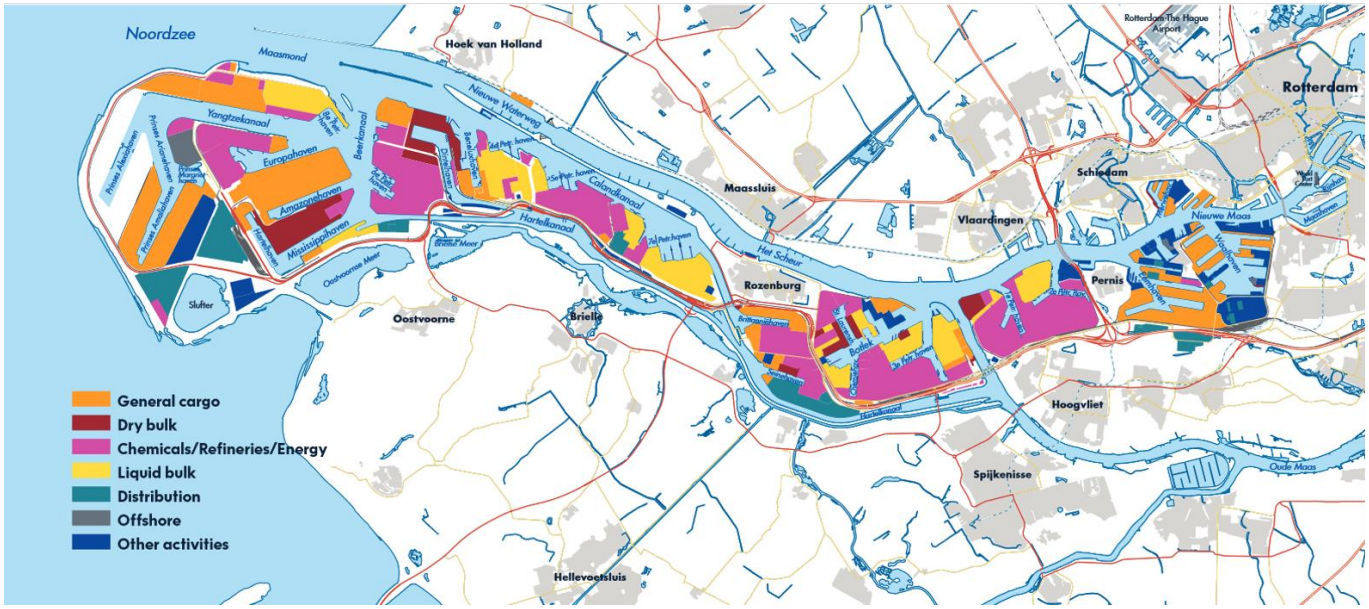

Figure 2.1.1. *Map of the city of Rotterdam, including the residential aeras (grey) and the harbour with industrial area's in coloured patches. Various colours are used to indicate different industrial activities.*

2.1.2 Campaign description

During August-September 2022 an intensive period of observations was conducted for fine scale urban mapping and hotspots characterization in the harbour (including ship emissions), industrial and domestic areas of the Rotterdam-Amsterdam (The Netherlands), in a campaign carried out in collaboration with the local authorities, the H2020-PAUL project, and the Ruisdael Observatory (see Figure 2.1.3 for the location of measurements).

The campaign efforts included:

- The involvement of representatives from the national (RIVM) and municipal (DCMR) air quality monitoring authorities for the provision of data from the permanent national and municipal AQMNs (Air Quality Monitoring Networks) and operational support;
- Ground-based fine scale mapping of aerosols (number and mass concentrations, ultra-fine particles (UFP), cloud condensation nuclei (CCN) black carbon (BC), brown carbon (BrC), concentrations, and chemical composition of atmospheric particulate matter (PM)) and gaseous pollutants (CO_2, CO, NO_2, CH_4, COS, C_2H_6, NO_2, NO, NOx, NH_3) using mobile and semi-mobile trailers, UUAQ car, and bicycles in specific routes.
- Temporary network of remote sensing instruments that included FTIR (Fourier Transform InfraRed) spectrometry for CO_2 and CH_4, wind lidar and 3 ceilometers for atmospheric dynamic and innovative air quality techniques (linked to T1.3), 2 MAX-DOAS (Multi-Axis Differential Optical Absorption Spectroscopy) observations for NO_2 and ship emissions.
- Two aircraft: first aircraft (6 flights) for in-situ airborne measurements of gasses and aerosols in and outside of the boundary layer over the city and adjacent suburban and rural areas; and a second aircraft (4 flights) equipped with TNO's Spectrolite instrument for mapping and satellite validation (TROPOMI - TROPOspheric Monitoring Instrument).

In parallel, measurements with cloud and rain radars, and microwave radiometers were conducted in the urban area, as well as in-situ and Raman lidar measurements at the Cabauw station (nearby rural area).

During the intensive period of observations, specific daily meetings and general weekly meetings were conducted for planning and evaluation of data quality.

RI-URBANS (http://www.RIURBANS.eu) is supported by the European Commission under the Horizon 2020 – Research and Innovation Framework Programme, H2020-GD-2020, Grant Agreement number: 101036245

2.1.3 Methodology

The approach of the campaign was to use stationary as well as mobile observations to map out the air pollution, including meteorological observations and vertical profiling of wind and aerosols. The underlying idea is that the full dynamics in an urban environment needs to be considered, which means that apart from the concentrations, the meteorological conditions need to be considered. Moreover, not only the ground level observations at the standard heights of 3.5 m above the ground should be taken, but as much as possible, also the vertical profile of wind as well as the vertical layering structure in the atmosphere. This is schematically depicted in Figure 2.1.2.

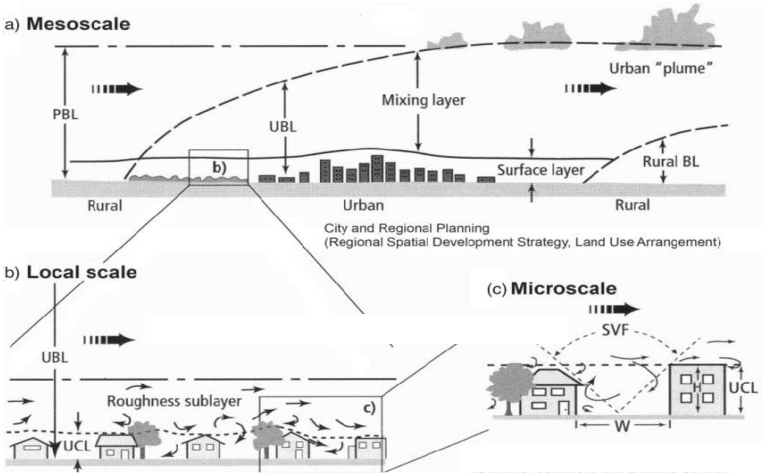

Figure 2.1.2. *Schematic of vertical structure in the atmosphere over an urban area at various spatial scales.*

The measurements were carried out inside the hot spot areas as well as further away from the emission sources. Furthermore, the Cabauw Atmospheric Research Station, that is located about 20 km towards the East from Rotterdam is located in a rural background and can therefore be used as a reference to see the background against which the pollution from the industrial activities can be seen. Moreover, a temporary station was located to the West of the harbour area to be above the prevailing wind, such that a relatively clean background could also be detected.

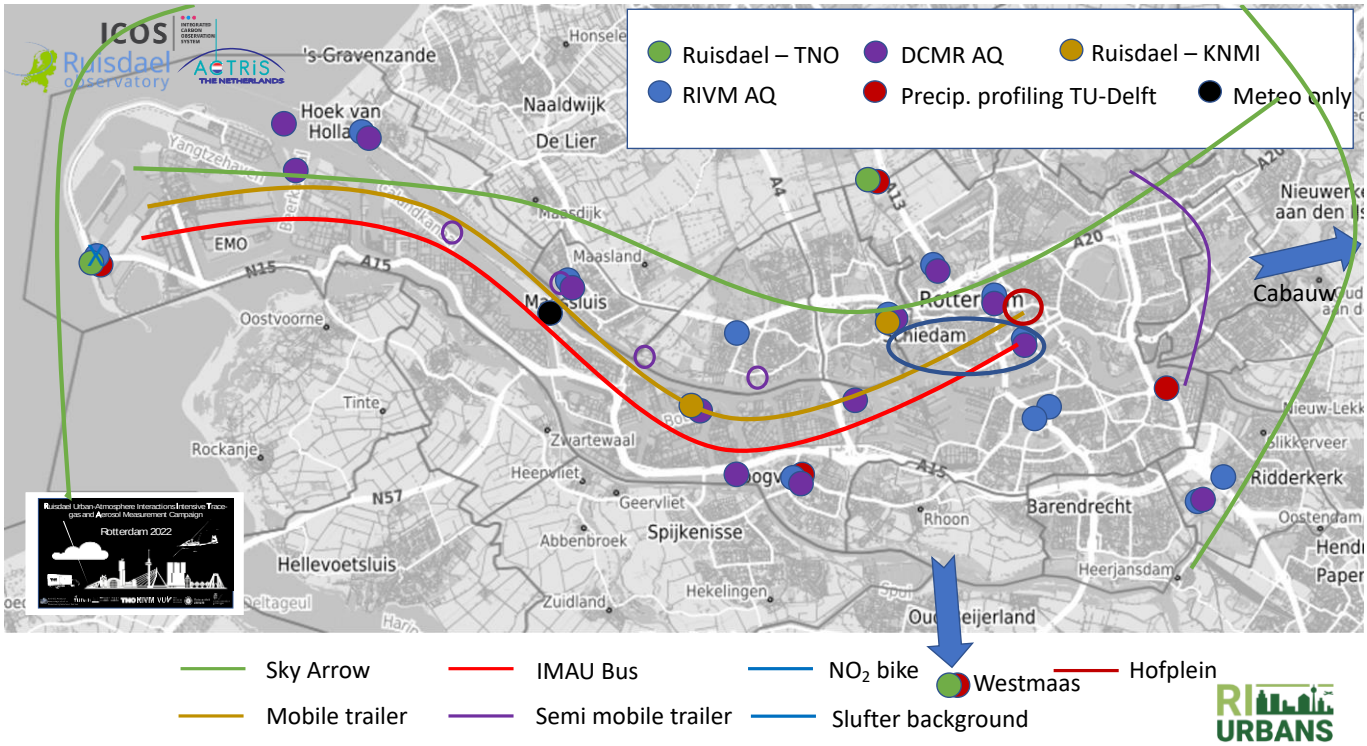

Figure 2.1.3. *Indication of observing stations and routes of mobile observations during the Rotterdam campaign.*

RI-URBANS (http://www.RIURBANS.eu) is supported by the European Commission under the Horizon 2020 – Research and Innovation Framework Programme, H2020-GD-2020, Grant Agreement number: 101036245

2.1.4 Observations

Since the suite of observations performed during the Rotterdam campaign is quite extensive, not all collected data can be shown, nor examples of all different types of observations. Therefore, it was decided to show a selection of the types of observations to illustrate how these are used to fulfil the goals for the campaign and how they contribute to the methodology.

Permanent stations

Data from the permanent stations are available from https://data.rivm.nl/data/luchtmeetnet/Vastgesteld-jaar/

Figures 2.1.4 to 2.1.6 show examples of the vertical profiling measurements with the wind lidar and ceilometers.

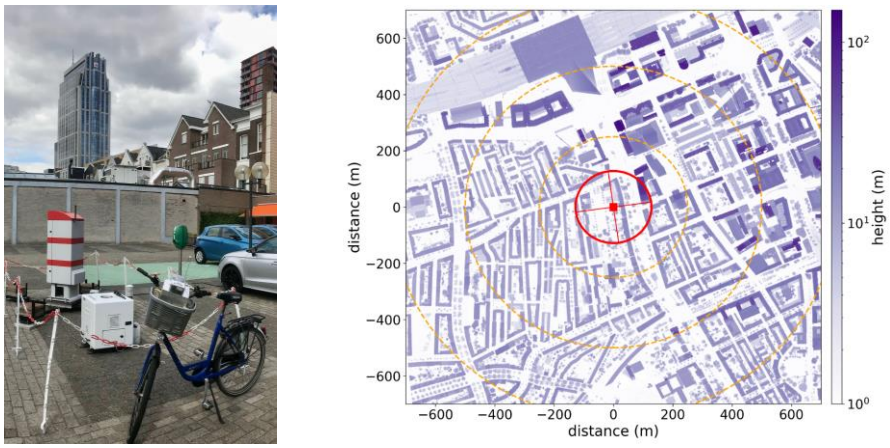

Figure 2.1.4. *Placement of a ceilometer and a wind lidar in the center of Rotterdam (left) and a map the height of the surrounding buildings within a 300 m radius (right). For orientation: the Rotterdam central railway station (Rotterdam CS) is in the top of the map.*

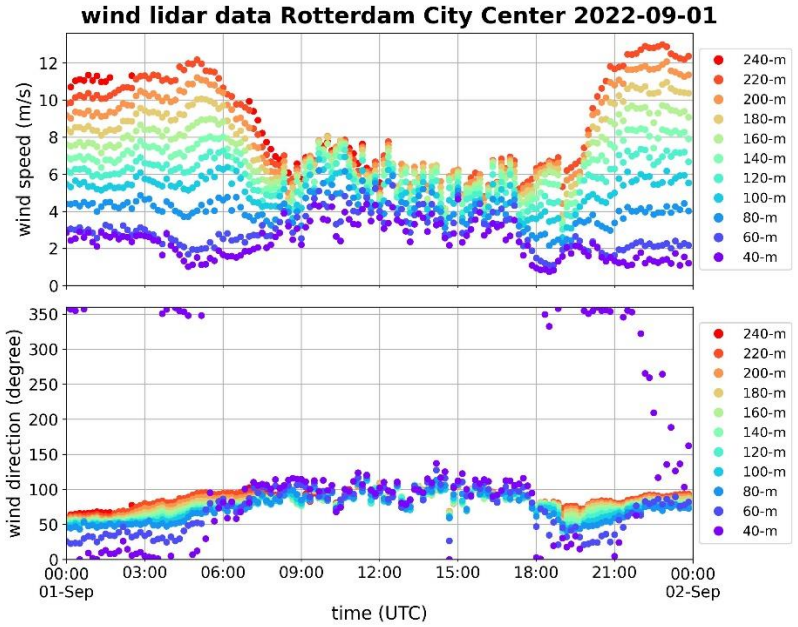

Figure 2.1.5. *Example of wind profile observations in the center of Rotterdam for a single day, 1 Sept. 2022.*

RI-URBANS (http://www.RIURBANS.eu) is supported by the European Commission under the Horizon 2020 – Research and Innovation Framework Programme, H2020-GD-2020, Grant Agreement number: 101036245

An example for 1 Sept. 2022 of the horizontal wind speed profile in the city centre of Rotterdam is shown in Figure 2.1.5. During daytime roughly between 7 AM and 7 PM (UTC) the wind profile shows much more similarity between 40 m and 240 m above ground level than during the night. This is a consequence of the growth of the boundary layer during the day due to rising warm air.

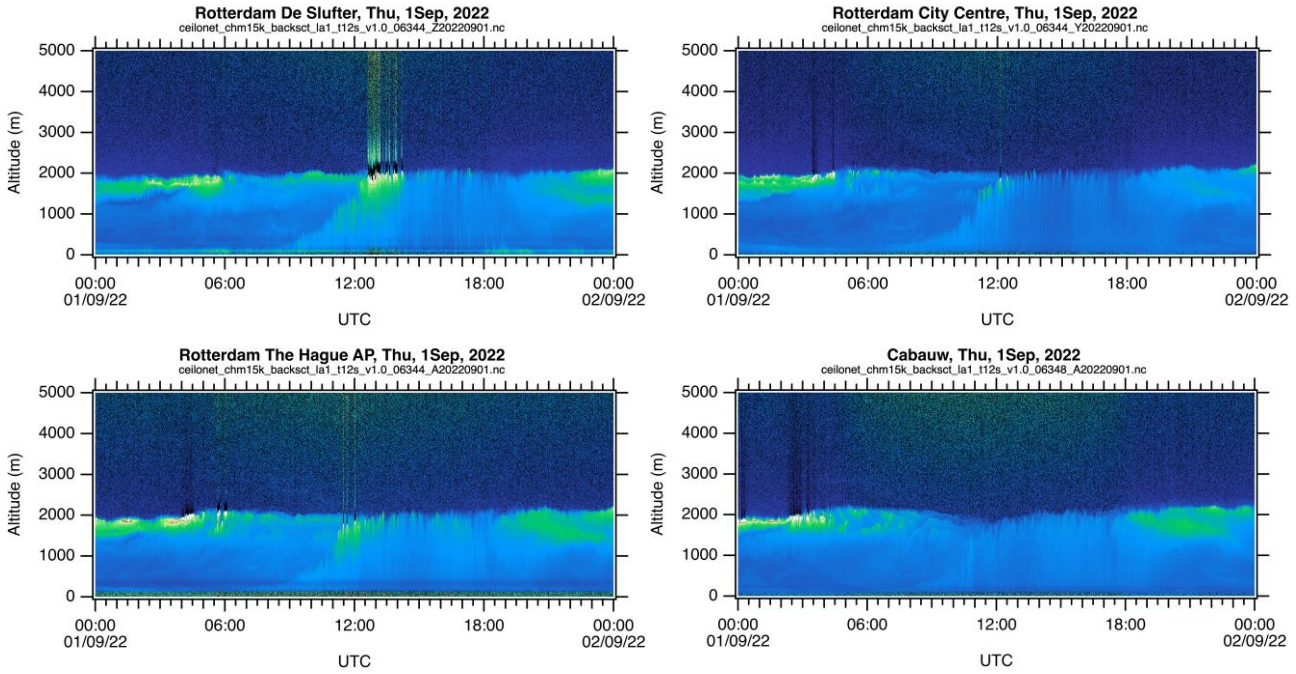

Figure 2.1.6. *Example of ceilometer observations for a single day, 1 Sept. 2022, at four locations in and around Rotterdam. From West 'De Slufter' to East 'Cabauw'. Refer to the map in Figure 2.1.3 for the locations. The ceilometer in the city center is co-located with the Doppler wind lidar shown in Figure 2.1.4.*

For the same day as in Figure 2.1.5, Figure 2.1.6 shows the vertical distribution of aerosols during the day at the measurement locations from West to East over the campaign area, including the Cabauw station to the East of Rotterdam. In the aerosol profiles the growth of the boundary layer can be seen from 7 AM (UTC) until mid-day. At the end of the day 7 PM (UTC) the rising motion of air stops, but the aerosols and pollution remain in a well-mixed layer up to about 2 km altitude.

Although the overall behaviour of the boundary layer is similar between the locations (the maximum depth reached is about 2 km for all stations as well as the time during the day when that happens), close inspection of the dynamics of the boundary layer height shows differences in behaviour between the stations. This is due to the local conditions of surface temperature and surface roughness.

The combination of the wind profiles, in the city (shown in Figure 2.1.5) and outside of the city (not shown here) together with the vertical distribution of aerosols as a proxy for air pollution provide essential information to analyse the dispersion of air pollution away from the hot-spots.

Mobile observations

Bicycle measurements.

In order to map the fine scale in in particular the contributions of road traffic in various parts of the city, an NO2 sonde was mounted on a bicycle along with a hand held aethalometer (BC). Since carrying out the measurements is very time consuming (labour intensive) citizens from Rotterdam were invited to volunteer for the bike rides. This was done on-line, as well as in a radio broadcast on a local radio station. Figures 2.1.7 and 2.1.8 show examples of

RI-URBANS (http://www.RIURBANS.eu) is supported by the European Commission under the Horizon 2020 – Research and Innovation Framework Programme, H2020-GD-2020, Grant Agreement number: 101036245

the measurements carried out with bicycles and citizens involvement. This resulted in 36 NO_2/BC measurements along the same ~20 km track. Form those, 25 successful NO_2 measurements were extracted: 1st week of NO_2 measurements was problematic, some of the data might be useful. All 36 BC measurements were successful.

Figure 2.1.7. *Bicycle operated observations of NO2 in Rotterdam, Sept. 2022.*

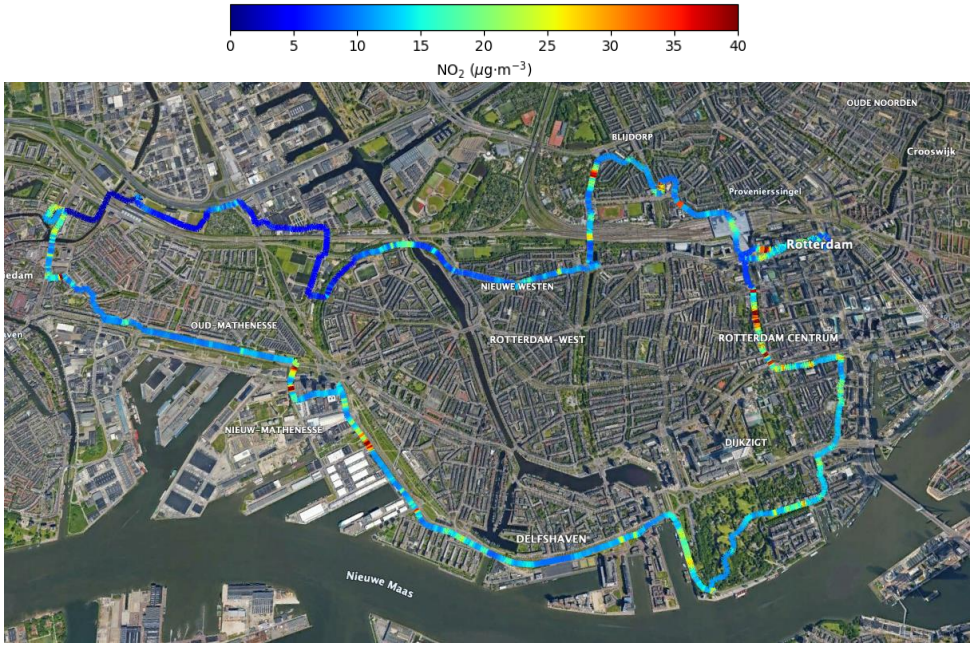

Figure 2.1.8. *NO_2 concentrations measured by citizens riding a bicycle equipped with a NO2 sonde that provides high time resolution measurements on August between 11:00-13:00 hours LT. Various local hot spots can be seen during the track.*

RI-URBANS (http://www.RIURBANS.eu) is supported by the European Commission under the Horizon 2020 – Research and Innovation Framework Programme, H2020-GD-2020, Grant Agreement number: 101036245

Airborne observations

An advanced airborne imaging spectrometer 'Spectrolite', build by TNO was deployed to map NO2 in high resolution over the city and harbour. The instrument was mounted on a Cessna Skyhawk (Figure 2.1.9 left) over a viewport in the bottom of the aircraft fuselage. Flight patterns were flown over the city at about 1500 m altitude in order to have the majority of the boundary layer and the pollution contained therein, within the atmospheric column below the aircraft.

An example of a measurement is shown in Figure 2.1.10 for 1st September 2022. This was a clear day without low clouds as can also be seen from the backscatter lidar observations (ceilometer) in Figure 2.1.6.

Figure 2.1.9. *The Spectrolite instrument mounted in a Cessna Skyhawk single engine aircraft (left) flying over the city and harbor/industrial area (right) to map NO_2 vertical column densities (VCD) (See Figure 2.2.10).*

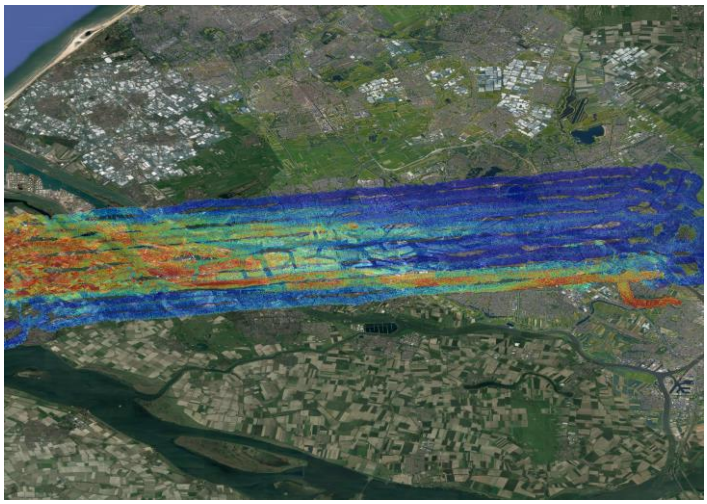

Figure 2.1.10. *Example of NO_2 Vertical Column Densities measured during a flight on 1 Sept. 2022. The more polluted area's associated with the harbor can be clearly distinguished (red and yellow colours) from cleaner rural areas to the East of the city (green and blue). Note that the Cabauw station is just outside the image to the East.*

RI-URBANS (http://www.RIURBANS.eu) is supported by the European Commission under the Horizon 2020 – Research and Innovation Framework Programme, H2020-GD-2020, Grant Agreement number: 101036245

Mobile trailer observations

Mobile trailer observations were used to map concentrations of various gaseous pollutants, as well as aerosols. The trailers are shown in Figure 2.1.11. In addition, a small car equipped with aerosol detectors are driven through the city and harbour area. These are not shown here.

An example of where hot spots of pollution can be found in the city is shown in Figure 2.1.12. In this figure simultaneous observations of N_2O and methane are shown.

Figure 2.1.11. *Mobile installations for air quality and greenhouse gas observations that have been driving around in the city and throughout the harbor and industrial area.*

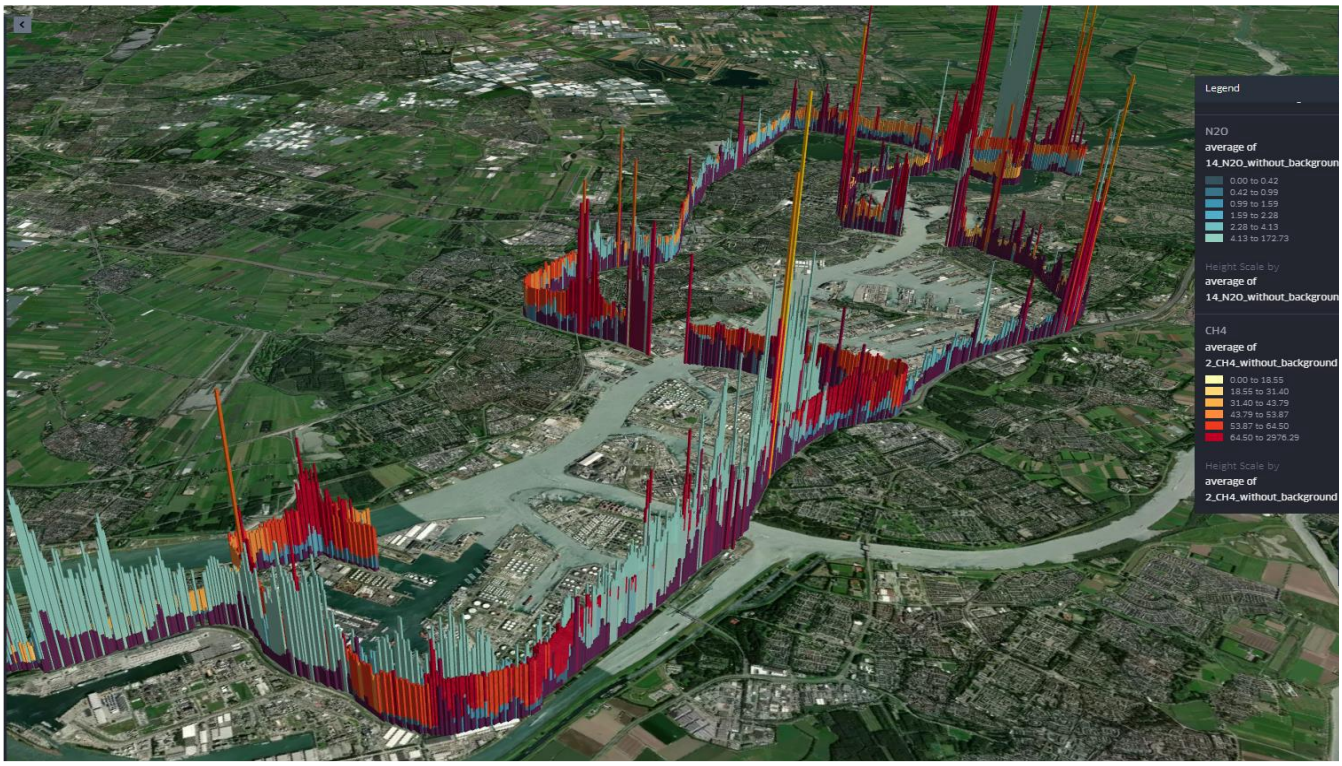

Figure 2.1.12. *Example of a track of the mobile observations of N_2O and CH_4. Along with the gas concentrations, air quality parameters such as aerosols were also measured (not shown). Various hot spots were detected.*

RI-URBANS (http://www.RIURBANS.eu) is supported by the European Commission under the Horizon 2020 – Research and Innovation Framework Programme, H2020-GD-2020, Grant Agreement number: 101036245

2.1.5 Modelling

In order to connect the observations to understanding of the existence of hot-spots and the dispersion of air pollution away from the sources of emission in a complex environment as a city with a neighbouring harbour and industrial aera, it is necessary to perform high resolution modelling within the urban canopy. This is challenging since the implementation of the urban canopy in high resolution models such as DALES (Delft Large Eddy Simulation) is relatively new. More traditional models can also be run at resolutions under 100 m. Extensive information on the vertical structure of the atmosphere including the meteorology is needed in order to understand the behaviour of the models. During the campaign this information was collected (see previous paragraphs).

In Figure 2.1.13 and example is given of an implementation of the urban canopy in Rotterdam. In this experiment an artificial emission was modelled and the dispersion of the source between the buildings was modelled. The still image on the right of Figure 2.1.13 is a single frame of an animation.

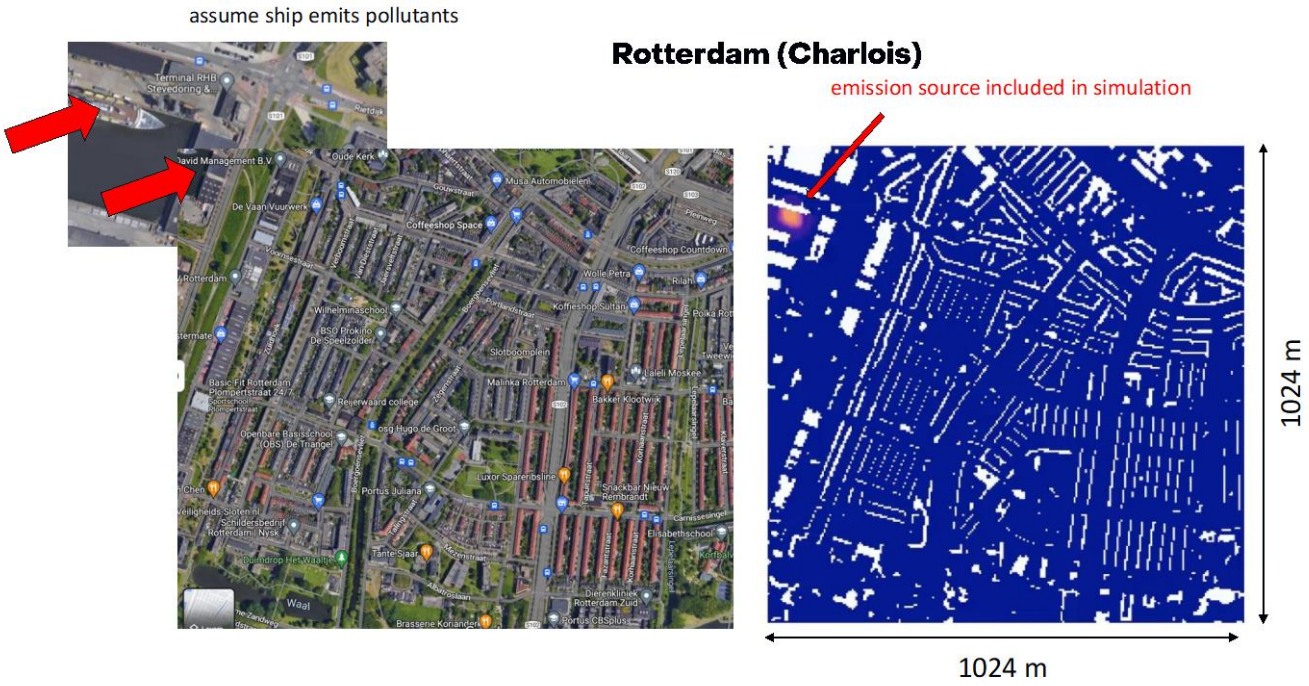

Figure 2.1.13. *Example of a LES simulation (DALES) of an emission from a ship close to a residential part of Rotterdam. The urban canopy was implemented into the model such that the spreading of the emission between the buildings could be simulated.*

2.1.6 Discussion and future work

A number of examples are shown of the extensive suite of observations that were made during the Rotterdam campaign addressing the hot spots in September 2022. From the overview of processed data that is obtained from the experiments it is expected that the intended results can be obtained. That is, using the fixed and mobile observations in and around the city, the influence and the extend of the hot spots can be analysed. We expect that the results from the Rotterdam campaign are sufficient to make a significant step in the modelling of the hot spots in state-of-the-art high-resolution models. This analysis is currently ongoing and further work will focus on interpretation and modelling.

RI-URBANS (http://www.RIURBANS.eu) is supported by the European Commission under the Horizon 2020 – Research and Innovation Framework Programme, H2020-GD-2020, Grant Agreement number: 101036245

2.2 Bucharest campaigns

2.2.1 About Bucharest

Bucharest, the capital of Romania, is located in the southern part of the country in the Romanian Plain. With a population of over 2.1 million in 2022 and 2.5 million in the metropolitan area (INSSE, 2024), it is Romania's largest city and its cultural, economic, and political center. Bucharest covers 240 km² and has a population density of over 9000 people per km². It has a diverse urban landscape with various types of land use, including industrial, commercial, and residential areas.

In Bucharest, the main sources of particulate matter pollution include road transport, industry and production processes, heating systems, construction and public works, agriculture, waste incinerators, as well as commercial and service activities. Road transport is one of the most significant sources of fine particulate emissions in Bucharest, mainly generated by vehicles using fossil fuels. Bucharest is considered 8th place in the world in traffic congestion (Tomtom, 2024). Bucharest city had a car fleet of 1,535,310 in 2022, out of which 80% were passenger cars. Among these, 59% were more than 10 years old.

Industry and manufacturing processes are another major source of pollution. In Bucharest are 29 large polluting companies, 3 landfills of which one is still active, and 2 water treatment plants according to Risk Management, within the National Environmental Protection Agency (ANPM, 2024). Also, the construction and public works generate dust and particles, in Bucharest are currently underway 377 residential construction sites, 16 industrial, 101 commercial, 127 community, 33 scientific/medical, 30 utility, and 79 infrastructures according to Bucharest City Hall.

Heating systems, especially those using fossil fuels or wood, are responsible for releasing particles into the air during the cold season (Guevara, 2016; Tomlin, 2021). In many areas of Bucharest, central heating with natural gas or solid fuel is a common practice. Among the various sources of particulate matter pollution in Bucharest, the CET West power plant stands out as a significant contributor. CET West is one of the largest thermal power plants in the city, providing a substantial proportion of Bucharest's electricity and heat supply.

2.2.2 About CET West power plant

CET West power plant (Figure 2.2.1), a vital energy provider for Bucharest, has been in operation since 1972, standing as a cornerstone of the city's power infrastructure. With an installed electrical power capacity of 436.25 MW and a formidable thermal power output of 1196 Gcal/h. Equipped with five steam turbines collectively capable of generating 310 MW, CET West ensures a steady supply of electricity to homes, businesses, and industries in the region (ELCEN, 2024). Operating on a flexible fuel system, it can run efficiently on either natural gas or fuel oil.

CET WWest has an imposing chimney reaching a height of 180 meters. In 2020, the plant underwent a significant modernization process, integrating advanced automation systems to enhance operational efficiency and sustainability.

Despite its modernization efforts, it remains one of Bucharest's significant industrial polluters (Figure 2.2.1), ranking as the second-largest emitter of particulate matter (PMs), nitrogen oxides (NOx), and carbon monoxide (CO) among energy providers, as well as the third-largest emitter of carbon dioxide (CO_2).

RI-URBANS (http://www.RIURBANS.eu) is supported by the European Commission under the Horizon 2020 – Research and Innovation Framework Programme, H2020-GD-2020, Grant Agreement number: 101036245

Figure 2.2.1 *Image of the hotspot area.*

2.2.3 Methodology

Scope and objectives of the pilot study

The focus of the Bucharest hotspot campaign was to assess the particle matter and NOx levels nearby a powerplant during high emission period and less intense heat generation capacity during the summer. The objective of the campaign includes the study of pollution levels at the reference site in a peri-urban area, with long-term measurements, and the same variables levels nearby the powerplant on a shorter timeframe. The most important question to be answered is if the study area is more polluted than the reference site and if the specific CET West power plant contributes to the pollution at near surface and high troposphere. Population exposure due to the power plant emission is a key factor for the residential areas nearby.

Observation strategy

Two strategies for measurements have been conducted in Bucharest using fixed and mobile measurements to reveal the pollution levels nearby the selected hotspot, CET West power plant (Figure 2.2.2).

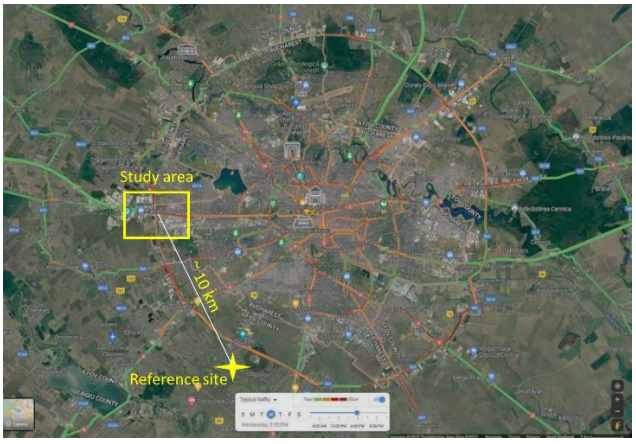

Figure 2.2.2 *Location of the two observation sites.*

A temporary observational site has been set up in May 2022 for in-situ and remote sensing observations in a highly polluted area near the CET West power plant. At the same time and with similar instruments have been conducted measurements at the permanent reference site (MARS), approximately 10 km southwest of the study area.

RI-URBANS (http://www.RIURBANS.eu) is supported by the European Commission under the Horizon 2020 – Research and Innovation Framework Programme, H2020-GD-2020, Grant Agreement number: 101036245

Simultaneously, mobile measurements of particle matter and NO_2 in a dense residential area close to the hotspot were conducted as part of the urban mapping task (T4.3).

2.2.4 The background reference site (MARS)

MARS (Măgurele center for Atmosphere and Radiation Studies, Figure 2.2.3) is a regional WMO-GAW station, providing specific data and analyses about sources in the south-eastern part of Europe. MARS, part of the RADO-Bucharest station, is an observational platform part of ACTRIS (44.344 N, 26.012 E, 77m). It is located in a peri-urban area, 8 km southwest of Bucharest and has three observational components: aerosol remote sensing, aerosol in situ, and cloud remote sensing.

MARS was established in 2020 on a 20,000 sqm flat terrain, it houses state-of-the-art atmospheric research instrumentation with five platforms for outdoor instruments. Indoor laboratories include ACTRIS-compliant aerosol remote sensing and aerosol in-situ components. The aerosol remote sensing laboratory is dedicated to aerosol properties proofing and employs RALI lidar and a sun/sky/lunar photometer. The Aerosol High-power Lidar unit of CARS comprise a laboratory for lidar optical blocks and components checks, providing specialized services for calibration and training in aerosol remote sensing instrumentation. The aerosol in-situ laboratory is dedicated to long-term aerosol properties studies, mainly aerosols chemical composition and physical characteristics at near surface. Outdoor laboratories include the ALPHA lidar, fixed reference in the framework of CARS, alongside other instruments on platforms and on the rooftop. ACTRIS-compliant cloud remote sensing focuses on studying cloud properties using instruments like cloud radar, microwave radiometer, and ceilometer. Another outdoor laboratory is the gas remote sensing, which utilizes Pandora - 2S and Mobile FTIR for ground-based measurements of ozone, nitrogen dioxide, and atmospheric composition. At MARS it is also measuring the micrometeorology, with a meteorological station, Doppler Sodar, Micro Rain Radar for comprehensive atmospheric condition analysis, and radiation, using a BSRN compliant station.

Main instruments used during this pilot studies are: Ceilometer, Wind lidar, lidar system, optical particle counter EDM180 Grimm.

Figure 2.2.3. *MARS observation site (background reference).*

2.2.5 The temporary observation site (INCAS)

INCAS temporary site (44.4351 N, 26.0043 E and 98m, Figure 2.2.4) is located in an urban area, nearby a high traffic area (approx. 200m) and CET West power plant (approx. 2.6Km). Also, a residential area from the North and East part influences the near-ground measurement at the site. Several instruments, similar with those measuring at

RI-URBANS (http://www.RIURBANS.eu) is supported by the European Commission under the Horizon 2020 – Research and Innovation Framework Programme, H2020-GD-2020, Grant Agreement number: 101036245

MARS, have been deployed stating May 2022 to this site: ceilometer, wind lidar, gas monitors, an optical particle counter (AQMesh sensor from Environmental Instruments monitors).

Figure 2.2.4. *INCAS observation site (temporary, near hotspot)*

The INCAS temporary site is about 2.6Km from the selected hotspot, with no high obstacles in between the site and power plant. Continuous measurements of the planetary boundary layer (PBL) height have been performed from this location (Figure 2.2.5).

The area is characterized by both industrial on the South and West side and residential on North and East side. The site is highly affected by the traffic, one of the most crowded roads in Bucharest is approx. 200m from the temporary site location.

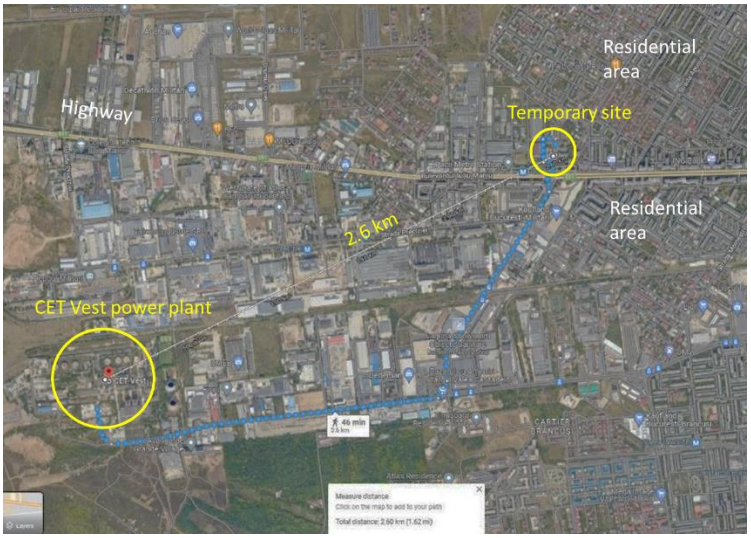

Figure 2.2.5 *Study area.*

2.2.6 Fine mapping with LUR model

The input data for the summer season were pollutant distribution maps with a horizontal resolution of 100 x 100 m from the summer measurement campaign conducted between May and July 2022. To achieve a fine resolution of 25 m for gridded data, a one-way two-level downscaling was used over the CET West Bucharest area. The pollutant distribution maps for the winter season were derived from the Random Forest (RF) regression model created in RI-URBANS, utilizing measurements taken during the winter campaign in the CET West region between January and February 2023. The downscaling technique and regression model were created in Python with dedicated machine learning tools (seaborn, scikit-learn, pandas, numpy, and matplotlib). To ensure data

RI-URBANS (http://www.RIURBANS.eu) is supported by the European Commission under the Horizon 2020 – Research and Innovation Framework Programme, H2020-GD-2020, Grant Agreement number: 101036245

consistency, the same predictors as during the summer season were used: land use (CORINE), traffic, and population density.

The NO_2, PM_{10}, and UFP maps were created for both seasons at a horizontal resolution of 25 x 25 m.

2.2.7 Results and discussions

Is the study area more polluted than the reference site?

Comparison between districts of Bucharest

Mobile measurements of ultrafine particle (UFP), $PM_{2.5}$, PM_{10}, and NO_2 have been performed in the frame of RI Urbans mapping task (T4.3), including also the residential area nearby the CET West and the CET West area. Averages of each pollutant representative for several Bucharest districts during the summer and winter periods are presented in Figure 2.2.6.

The results show that PM_{10} and $PM_{2.5}$ double their values during the cold season in all districts, while UFP concentrations slightly increase. NO_2 concentrations are higher during summer than during winter, probably associated to more intense traffic. The district where CET WestWest is located shows no significantly larger values compared to other districts during summer for UFP and NO_2, although higher values are measured for PM_{10} and $PM_{2.5}$. During the cold season, concentrations measured near CET West are amongst the highest for Bucharest, especially for PM_{10} and $PM_{2.5}$

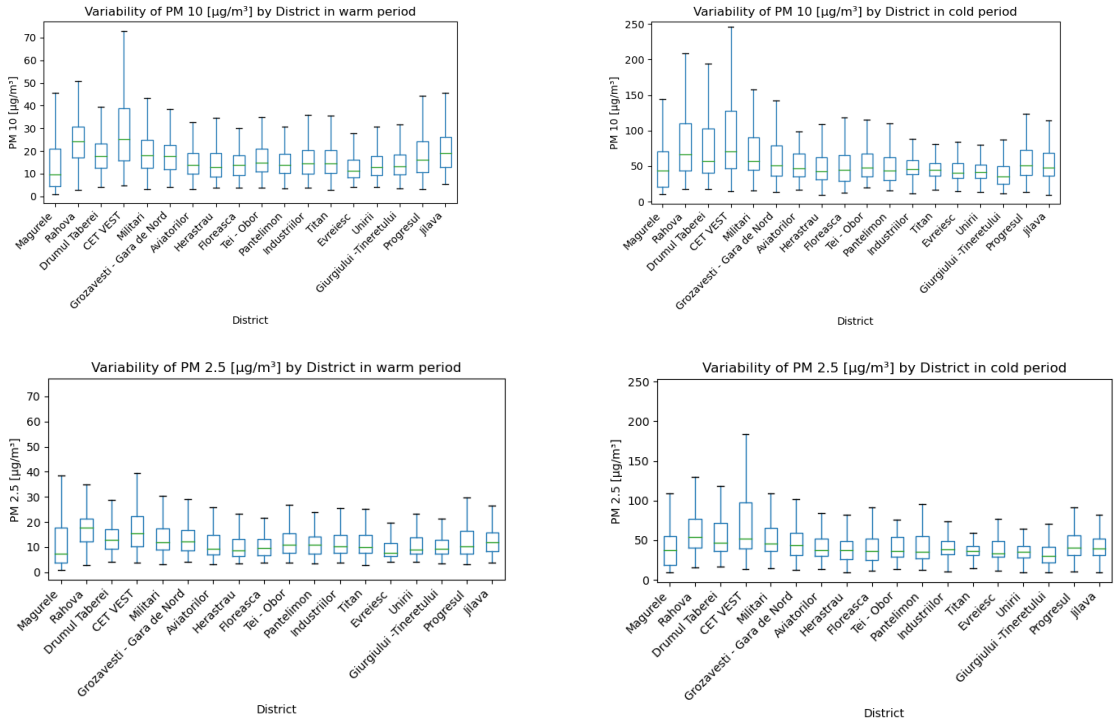

RI-URBANS (http://www.RIURBANS.eu) is supported by the European Commission under the Horizon 2020 – Research and Innovation Framework Programme, H2020-GD-2020, Grant Agreement number: 101036245

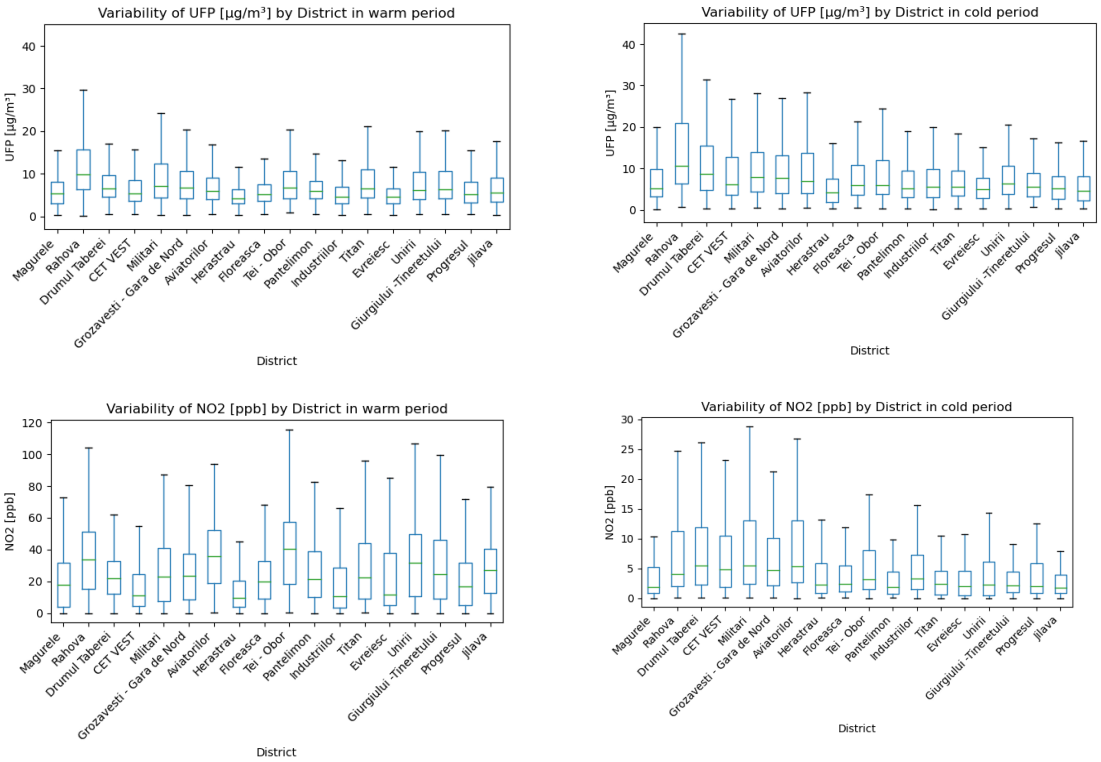

***Figure 2.2.6**. Average season near-surface concentrations at different Bucharest districts as observed by mobile measurements: a) PM_{10}; b) $PM_{2.5}$; c) UFP; d) NO_2 concentrations. Left panels: warm season; Right panel: cold season.*

Comparison between the two measurement sites

Aerosol near-surface data collected in the 2022 (May-August) with two similar optical particle counters can be analyzed from the perspective of air quality, to identify special events with increased mass concentrations of particle matter: PM_1, $PM_{2.5}$ or PM_{10}. According to European and national legislation regarding air quality the limit values of daily averages for PM_{10} and limit values for annual averages of PM_{10} and $PM_{2.5}$ are 50 µg/m^3, 40 µg/m^{3}and 25 µg/m^3 respectively (Air quality directive 2008/EC/50). The daily concentrations of PM_1, $PM_{2.5}$ and PM_{10} presents a similar variability and emphasize the presence of increased concentrations in July at both sites, with higher values in Magurele (MARS) for PM_{10} and important relative difference during local pollution events (Figures 2.2.7 and 2.2.8). The fine particle (PM_1) dominates at the temporary site in Bucharest (INCAS) during the entire period, while the bigger particles dominate the MARS location (Figures 2.2.9 and 2.2.10).

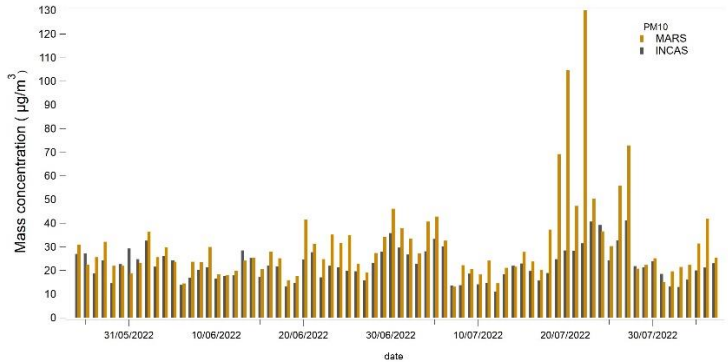

***Figure 2.2.7**. Variability of PM_{10} daily mass concentration at INCAS and MARS.*

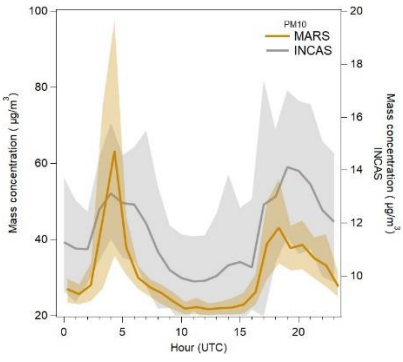

***Figure 2.2.8**. Diurnal pattern of PM_{10} at MARS and INCAS: average hourly values over the entire campaign.*

RI-URBANS (http://www.RIURBANS.eu) is supported by the European Commission under the Horizon 2020 – Research and Innovation Framework Programme, H2020-GD-2020, Grant Agreement number: 101036245

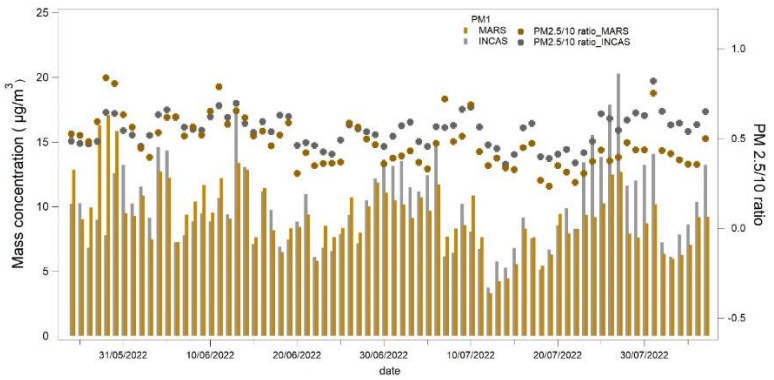

Figure 2.2.9 *Variability of PM1 daily mass concentration at MARS and INCAS (solid bars), and daily ratio PM2.5 to PM10 (points) at the same locations.*

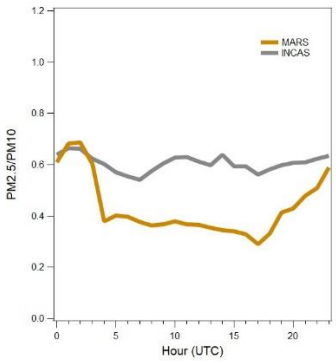

Figure 2.2.10. *Diurnal pattern of the ratio PM2.5 to PM10 at MARS and INCAS: average hourly values over the entire campaign.*

The PM_{10} daily mass concentration ranged between 13 and 132 µg/m^3 at MARS, and between 11 and 41 µg/m^3 at INCAS, nearby hotspot (Figure 2.2.7). In summer PM_{10} values were below the limits most of the time, with higher values at MARS usually. Only 6 exceedances of the daily threshold value for PM_{10} were noticed for the background reference site (MARS), but the particle variability is similar for the 2 sites.

Figure 2.2.8 presents the diurnal pattern of PM_{10} at both measurements' sites, with overall higher hourly mean values at the background site. Two peaks are highlighted in the diurnal cycle, corresponding with traffic rush hours (UTC) and decrease of the planetary boundary layer. A sharper peak characterizes MARS location (Magurele) in the morning, while a broader one characterizes INCAS location (Bucharest) due to extended traffic activity in the area. Evening peaks are broader than in the morning for both locations, and inverse correlate with the planetary boundary layer height, but still the more homogeneous traffic activity in the city is captured. An unexpected peak is present during the mid-day in Bucharest, which can be associated only with the traffic. For the warm period it was noticed the predominance of fine particles nearby hotspot, in contrast with the reference site, due to the nearby emission sources.

The PM_1 daily mass concentration ranged between 3.32 and 17.08 µg/m^3 at MARS, and between 3.75 and 20.30 µg/m^3 at INCAS (Figure 2.2.9). In summer PM_1 daily values were below 15 µg/m^3 most of the time, with higher values at INCAS usually. The particle variability was similar for the 2 sites, but the daily concentration for PM_1 was 19 times higher at INCAS with at least 2 µg/m^3 comparing to MARS. The ratio of $PM_{2.5}$ to PM_{10} daily concentrations (Figure 2.2.10, dots) are generally higher at INCAS than MARS, which means that small particles contribute more than at the background site. Small particles are associated to traffic and industrial sources, both being important at INCAS temporary site. Due to the vicinity of the western city exit to the highway, is impossible to estimate how much this pollution is due to the power plant, and how much due to traffic. A good indicator is the diurnal cycle of the $PM_{2.5}$ to PM_{10}, which should indicate the morning and evening rush hours if the traffic predominates.

The traffic-related peaks are visible in the diurnal cycle of the ratio $PM_{2.5}$ to PM_{10} (Figure 2.2.10) at MARS. At INCAS, close to the hotspot, there is no clear diurnal cycle, leading to the assumption that the hotspot is a constant source of smaller particles, overlaying to traffic-originated particles.

RI-URBANS (http://www.RIURBANS.eu) is supported by the European Commission under the Horizon 2020 – Research and Innovation Framework Programme, H2020-GD-2020, Grant Agreement number: 101036245

Does CET West contribute to the pollution at near surface?

2.2.8 Distribution of NO_2 and aerosol in the area

Figures 2.2.11 to 2.2.13 depict the results for the fine mapping of the study area during warm season (left panels) and cold season (right panels). Results are presented overlayed with the land use maps (upper panels) but also as gradient masks (lower panels) to put in evidence where high concentrations are observed and which areas are affected.

The hotspot does not seem to contribute significantly to the NO_2 concentrations (Figure 2.2.11), at least not during the warm season. Intense traffic at the western exit of the city is the primary source in the region. During the cold season, however, the power plant generates higher concentrations (see the right lower panel), while the residential heating becomes also important in the study area.

The situation is different for particles.

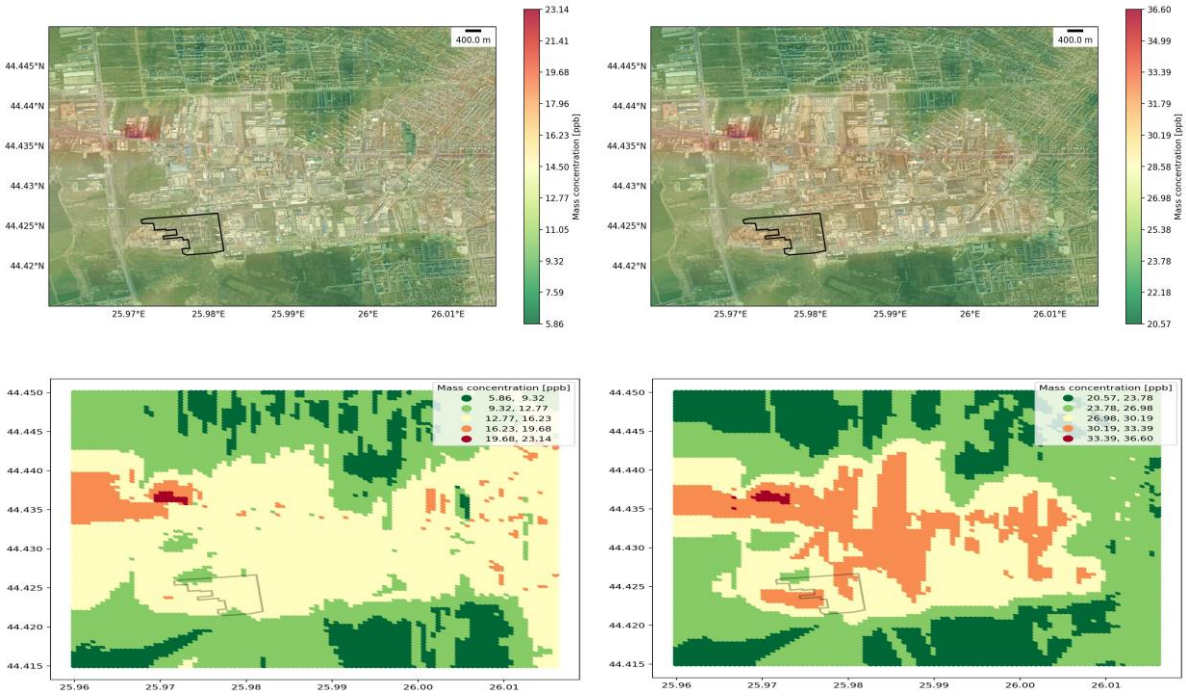

Figure 2.2.11. *NO_2 distribution over West-Bucharest area: summer (left panels); winter (right panels); overlay with land use map (top panels); gradient mask (bottom panels). The location of the power plant is marked with black contour.*

PM_{10} and UFP concentrations are more homogeneously distributed over the district. PM_{10} (Figure 2.2.12) presents higher values during winter but also higher gradients during summer (left panels), with large values over the residential area and at the entrance of the highway. These high concentrations of PM_{10} are associated to road dust, produced by construction and agricultural works, and transported by traffic. The power plant has no important roads in its vicinity and is not a source of large particles itself. The elevated planetary boundary does not favor horizontal mixing. During winter (right panels) the distribution of PM_{10} is much more homogeneous. This is because the planetary boundary layer is much lower, and mixes the particles lifted in the air. The entrance to highway is still visible as an important source, but the particles produced by the small and dense roads within the residential area and in the vicinity of the power plant are well mixed and distributed over the entire region.

RI-URBANS (http://www.RIURBANS.eu) is supported by the European Commission under the Horizon 2020 – Research and Innovation Framework Programme, H2020-GD-2020, Grant Agreement number: 101036245

In case of UFP (Figure 2.2.12), only slightly higher concentrations are measured during the cold season. UFP are generally associated to traffic and industry, but these small particles are also easily transported to large distances.

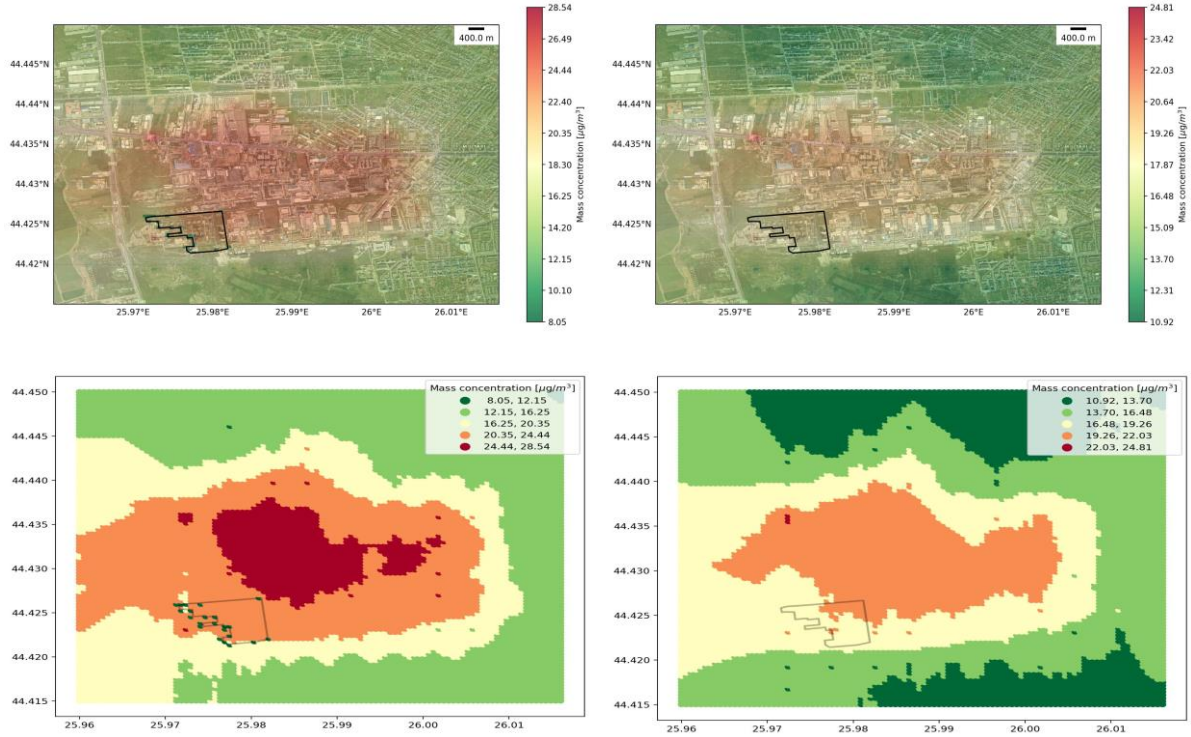

Figure 2.2.12. *PM_{10} distribution over West-Bucharest area: summer (left panels); winter (right panels); overlay with land use map (top panels); gradient mask (bottom panels). The location of the power plant is marked with black contour.*

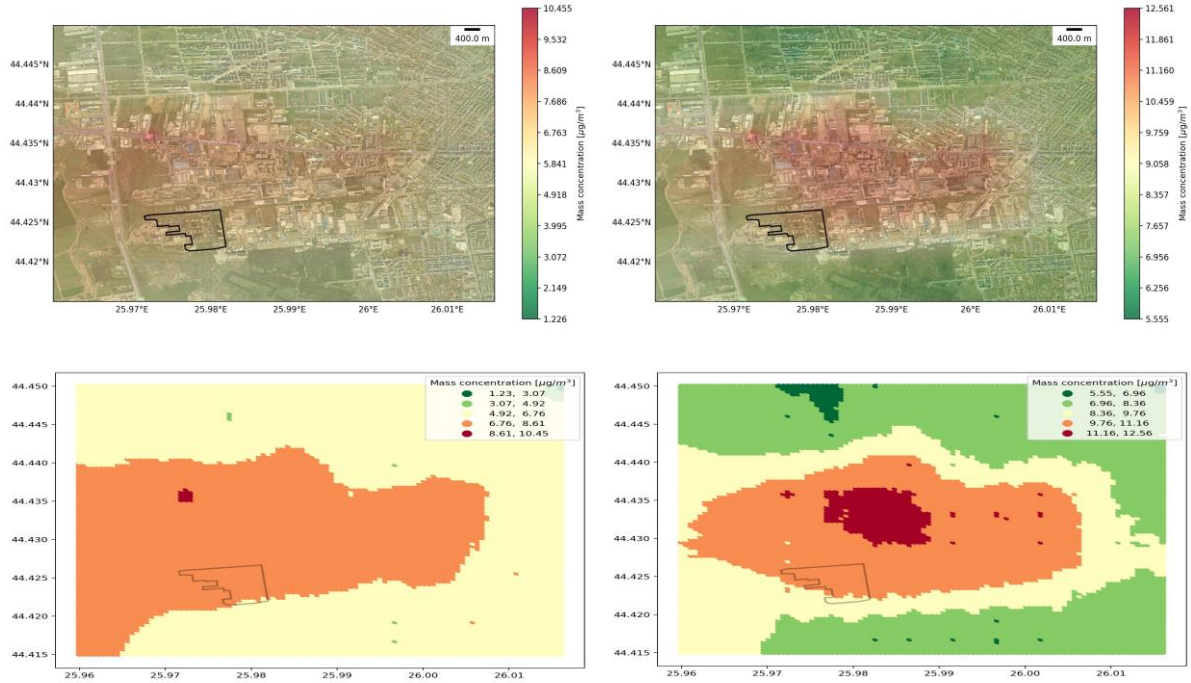

Figure 2.2.13. *UFP distribution over West-Bucharest area: summer (left panels); winter (right panels); overlay with land use map (top panels); gradient mask (bottom panels). The location of the power plant is marked with black contour.*

RI-URBANS (http://www.RIURBANS.eu) is supported by the European Commission under the Horizon 2020 – Research and Innovation Framework Programme, H2020-GD-2020, Grant Agreement number: 101036245

During summer (left panels) UFP are well distributed over the entire region, including over the power plant and the west of Ilfov county (pre-urban and rural areas surrounding Bucharest city). Traffic seems to be the predominant source of UFP, which is visible as a "hotspot" at the western exit of the city to highway, both during summer and winter. During winter, however, residential heating is also noticeable (right panels). The power plant does not seem to be a significant source of UFP.

2.2.9 Typical air mass circulations

To assess the impact of the CET West hotspot on air quality in Bucharest's western sector, we examined the circulation types of air masses in both the lower troposphere (850 hPa) and the middle troposphere (500 hPa).

Figure 2.2.14**Figure** depicts the wind rising during the summer season (left panel) and the winter season (right panel). The wind rising depicts wind speed and direction divided into eight classes (N, NE, E, SE, S, SW, NW, and N), with a 45° difference between each class.

Figure 2.2.14 shows that, except for the circulation of air masses from the middle troposphere in the cold season, which was dominated by a circulation from the southern sector (SE-S-SW), the western region of Bucharest was dominated by a circulation from the northern sector. The wind speed in the low troposphere varies greatly between 8 and 18 m/s in the summer, with an average of 12 m/s, however in the winter, the variance is narrower, ranging from 8 to 12 m/s with an average of 10 m/s.

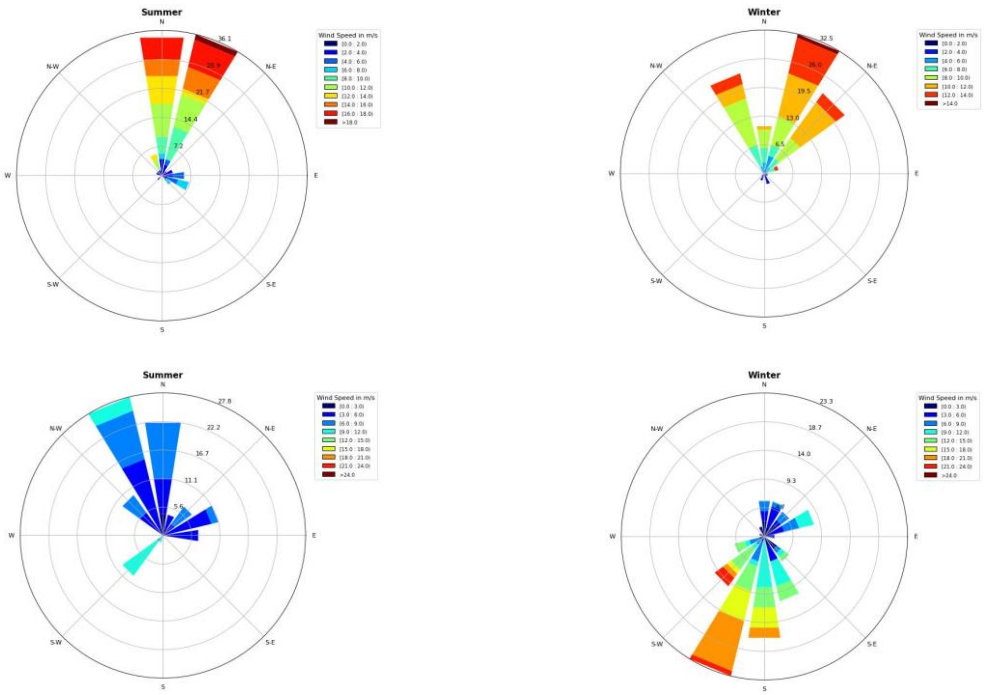

Figure 2.2.14. *Wind rose over West-Bucharest region: Summer in the left panels: pressure level at 850 hPa (up) and pressure level at 500 hPa (bottom) and winter in the right panels: pressure level at 850 hPa (up) and pressure level at 500 hPa (bottom)*

The analysis above shows that CET West is well located with reference to the residential area. Low wind speed would not favor the transport of pollutants, while predominant wind direction in the planetary boundary layer would transport the pollutants out of the city. The only situation which would favor the transport of pollutants from the power plant to the residential area is during winter nigh time, when the planetary boundary layer is very low, the pollutants are injected above and transported by mid-tropospheric winds from the southern sector (SE-S-SW).

RI-URBANS (http://www.RIURBANS.eu) is supported by the European Commission under the Horizon 2020 – Research and Innovation Framework Programme, H2020-GD-2020, Grant Agreement number: 101036245

2.2.10 Mixing Layer Height

The ceilometer data have been analyzed as averaged values representative for summer and autumn, June-November 2022, to assess the mixing layer height (MLH). The seasonal diurnal cycles for MLH are represented in Figure 2.2.15. The median MLH at both locations during summer is approximative 2500 m, and during autumn approximative 1000 m. The hourly average of MLH is higher at INCAS location on both seasons during the entire day. It can be noticed difference on the maximum MHL, for example on autumn the maximum MLH for INCAS is reached around 14 UTC, while for MARS one hour later. This behavior is favorized by the urban heat island in the city.

The minimum MLH is reached during night time (23:00 – 05:00 UTC) and is below 400 m (the measurement limit of the ceilometer, i.e. the full overlap) for both seasons. Unfortunately, we cannot say, based on the ceilometer measurements, if the MLH ever goes down to 150 m (below the 180 m height of the CET West chimney). Tilted lidar measurements will be needed.

Figure 2.2.16 shows the mean diurnal cycle of the attenuated backscatter profile for summer and autumn at MARS and INCAS emphasizing similar patterns for both locations on the same season. Higher values of attenuated backscatter profile are observed in the case of INCAS location for both planetary boundary layer and troposphere. The presence of more particles in the PBL is observed on all seasons and locations. Also, middle, low-level and high-altitude clouds are observed at both locations with more intensity in Bucharest during summer period.

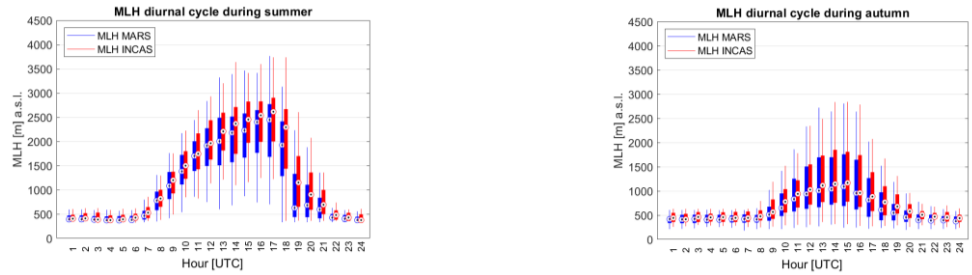

***Figure 2.2.15**. Diurnal cycle for MLH for the warm (left panel) and cold seasons (right panel) at MARS and INCAS*

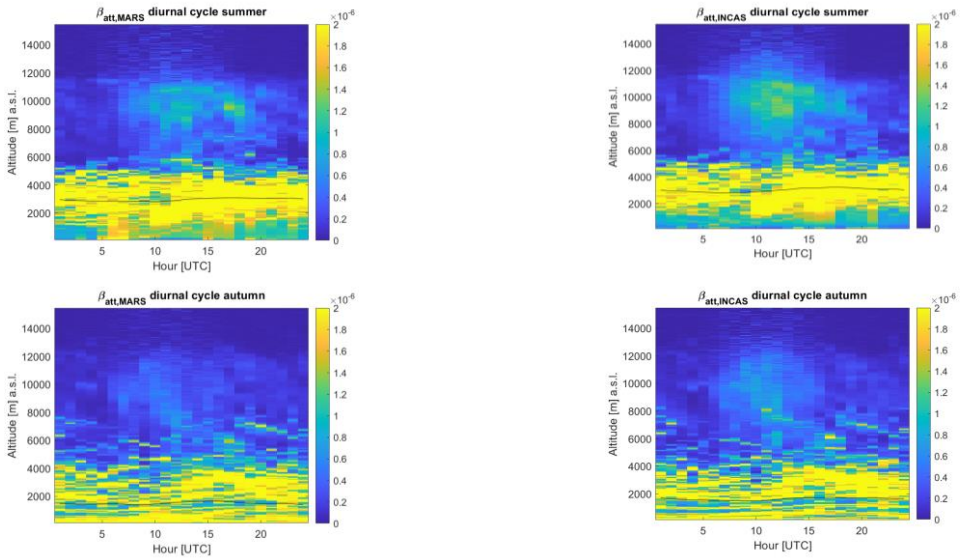

***Figure 2.2.16.** The diurnal cycle for attenuated backscatter coefficient: summer (upper panels) and autumn (lower panels). The black line represents the diurnal PBLH.*

RI-URBANS (http://www.RIURBANS.eu) is supported by the European Commission under the Horizon 2020 – Research and Innovation Framework Programme, H2020-GD-2020, Grant Agreement number: 101036245

2.2.11 Conclusions and future work

CET West power plant has been in operation since 1972, it can run efficiently on either natural gas or fuel oil, has an imposing chimney reaching a height of 180 meters, and underwent a significant modernization process in 2020. Despite its modernization efforts, according to the reports of the National Environmental Agency, CET West it remains one of Bucharest's significant industrial polluters, ranking as the second-largest emitter of particulate matter (PMs), nitrogen oxides (NOx), and carbon monoxide (CO), as well as the third-largest emitter of carbon dioxide (CO_2) among energy providers.

In this study we present our findings regarding the potential adverse effect of the CET West on the population living in the nearby residential area, northeast the power plant. Note that the western district of Bucharest (our study area) is a complicated region with many important pollution sources, from constructions, industry, traffic and even agriculture. As such, decoupling the impact of the power plant from the impact of other sources is not completely possible, for two reasons: a) measurements and measured-based modelling embed contributions from all sources – separation can only be qualitatively made; b) publicly available emission inventories for Bucharest are not trustable, e.g. constantly underestimating traffic, therefore inventory-based modelling gives unrealistic outputs. We preferred to base our study on observations.

Based on the analysis above, our expectations that the CET West power plant could be affecting the air quality in the residential areas nearby is not confirmed. The only pollutant which can localize the power plant as a source is NO_2, mostly during winter (note that CO_2 and CO measurements were not available for this study). NO_2 is a highly reactive gas, therefore it is destroyed before being transported to the residential areas, so is only affecting the very small region around the power plant.

CET West is not a significant source of particles, not even UFP. Higher concentrations of PM_{10} and $PM_{2.5}$ have been measured near the power plant, but the differences to other districts are not sufficiently large to allow a clear identification of the source. Road dust produced by agricultural and construction works and transported by traffic is always present, hiding the contribution of the power plant up to a point. The fact that the differences to other districts are higher during the cold season may indicate that the power plant is a constant source of particles in the region (the power plant increases its operations during winter). However, it does not mean that people living northeast of CET West are affected by it.

CET West is well located with reference to the residential area. Low wind speed would not favour the transport of pollutants, while predominant wind directions in the planetary boundary layer would transport the pollutants out of the city. The only situation which would favour the transport of pollutants from the power plant to the residential area is during winter night time, when the planetary boundary layer is very low, the pollutants are injected above and transported by mid-tropospheric winds from the southern sector (SE-S-SW). The minimum MLH is reached during night time (23:00 – 05:00 UTC) and is below 400 m (the measurement limit of the ceilometer, i.e. the full overlap) for both seasons. Unfortunately, we cannot say, based on the ceilometer measurements, if the MLH ever goes down to 150 m (below the 180 m height of the CET West chimney). Tilted lidar measurements will be needed and will be organized in the second part of the study to clarify this aspect.

2.2.12 References

National Institute of Statistics (INSSE), Populatia, https://bucuresti.insse.ro/. Last accessed 08-02-2024.

He, L. Y., Hu, M., Zhang, Y. H., Huang, X. F., & Yao, T. T. (2008). Fine particle emissions from on-road vehicles in the Zhujiang Tunnel, China. Environmental science & technology, 42(12), 4461-4466.

Kousoulidou, M., Ntziachristos, L., Mellios, G., & Samaras, Z. (2008). Road-transport emission projections to 2020 in European urban environments. Atmospheric Environment, 42(32), 7465-7475.

RI-URBANS (http://www.RIURBANS.eu) is supported by the European Commission under the Horizon 2020 – Research and Innovation Framework Programme, H2020-GD-2020, Grant Agreement number: 101036245

Tomtom, Traffic Index ranking, https://www.tomtom.com/traffic-index/ranking/, Last accessed 08-02-2024.

Munsif, R., Zubair, M., Aziz, A., & Zafar, M. N. (2021). Industrial air emission pollution: potential sources and sustainable mitigation. In Environmental Emissions. IntechOpen.

Agentia Nationala de protectia Mediului (ANPM), SEVESO, https://www.anpm.ro/ro/managementul-riscului-seveso, Last accessed 08-02-2024.

Guevara, M. (2016). Emissions of primary particulate matter.

Tomlin, A. S. (2021). Air quality and climate impacts of biomass use as an energy source: A review. Energy & Fuels, 35(18), 14213-14240.

Wu, Z., Zhang, X., & Wu, M. (2016). Mitigating construction dust pollution: State of the art and the way forward. Journal of cleaner production, 112, 1658-1666.

Klimont, Z., & Brink, C. (2004). Modeling of emissions of air pollutants and greenhouse gases from agricultural sources in Europe.

Knorr, W., Dentener, F., Lamarque, J. F., Jiang, L., & Arneth, A. (2017). Wildfire air pollution hazard during the 21st century. Atmospheric Chemistry and Physics, 17(14), 9223-9236.

Challoner, A., & Gill, L. (2014). Indoor/outdoor air pollution relationships in ten commercial buildings: PM2. 5 and NO2. Building and Environment, 80, 159-173.

Drăgan, M., & Munteanu, G. (2021). LANDFILL FIRES IN ROMANIA. Riscuri si Catastrofe, 29(2).

ELCEN, Electrocentrale Bucureşti, https://www.elcen.ro/#/home, Last accessed 08-02-2024.

RI-URBANS (http://www.RIURBANS.eu) is supported by the European Commission under the Horizon 2020 – Research and Innovation Framework Programme, H2020-GD-2020, Grant Agreement number: 101036245

2.3 Po Valley (Milano) campaign

2.3.1 Milan city and metropolitan area

The city of Milan is located in northern Italy (45°28'01"N 09°11'24"E, Figure 2.3.1.), with a population of 3.22 million citizens it is considered the second most populated city in Italy after the capital Rome. The population of the wider Milan metropolitan area (including the urban centres of Milan, Monza, Como, Lecco extending to the North) is estimated to be between 4.9 million and 7.4 million, which makes Milan the largest metropolitan area in Italy and one of the largest in the European Union.

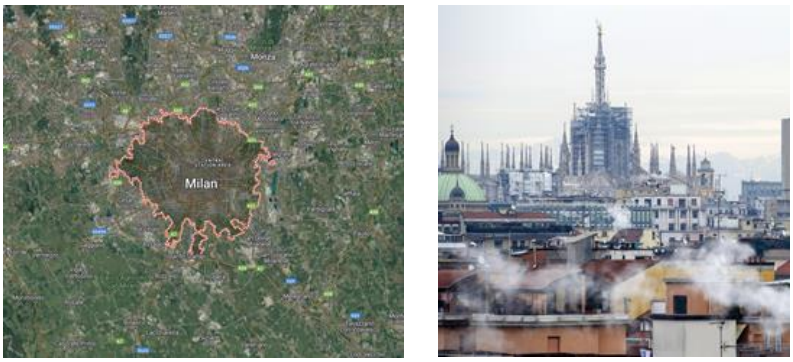

Figure 2.3.1. *Left: Satellite view of Milan (google maps). Right: Wintertime atmospheric pollution in the urban area.*

Milan is also an economic, cultural and touristic center in Italy, with many industries and universities located within the metropolitan area. The surrounding area of the metropolitan Milan is the rural Po Valley, a flat area hosting intense farming activities. Milan is located in the north-western section of the Po Valley, halfway between the Po river to the South and the Alps to the North, with the highest site in the city located at 122 m above sea level. The Alps in the North and the Apennine mountains in the South form a natural barrier to the area reducing the air ventilation and causing the atmospheric pollutants emitted from the urban as well as the rural areas to concentrate within the valley, which often experiences severe pollution episodes, mostly during wintertime. The climate in Milan is characterized by hot and humid summers and cold foggy winters, with very mild winds due to the particular geographic location. Transport within the metropolitan area and outside of it is organized through a network of underground, suburban, national and international rail system, buses and trams, three airports, one of which (Milano Linate) located inside the city, and a cycling network comprising about 300 km of bike lanes (La Repubblica, April 2023). It is estimated that for every 10 inhabitants of Milan, 8.9 private cars circulate in the city (a total of 2.73 million compared to a population of 3.02 million in 2017). Among the 2.73 million cars registered in 2017, 47% are fueled with gasoline, while 43% use diesel, and the others are hybrid (Sole 24 ore, February 2020). Previous studies conducted in the urban and metropolitan area of Milan showed that $PM_{2.5\ and}$ PM_{10} mass concentrations have a strong seasonal variability, with higher values reported in wintertime. Traffic and secondary aerosols (also originated from traffic) were found to be the largest contributing sources of $PM_{2.5\ and}$ PM_{10} (Marcazzan et al., 2003). The organic aerosol fraction largely composing PM_{10} was studied in detail afterwards. Combining measurements with model results it was showed that residential heating biomass burning primary organic aerosols was the dominant source during wintertime contributing to the organic fraction, while secondary organic aerosol mostly originating from traffic, industry, energy production, shipping as well as biogenic emissions dominate the summertime organic fraction (Daellenbach *et al*., 2023).

RI-URBANS (http://www.RIURBANS.eu) is supported by the European Commission under the Horizon 2020 – Research and Innovation Framework Programme, H2020-GD-2020, Grant Agreement number: 101036245

2.3.2 Milano Linate international city airport hot-spot of pollution

Milano Linate international airport is the city airport located about 7 km East of the city center (45° 26' 34.79" N, 9° 16' 25.20" E, Figure 2.3.2). It is the third busiest airport in the Milan metropolitan area in terms of passenger numbers after Malpensa Airport and Orio al Serio Airport and the second busiest in terms of aircraft movements. It mainly serves domestic, short distance and international flights within Europe.

Linate airport has one terminal building with several facilities, including restaurants, shops, passenger and service facilities. Ground transport to the airport is possible by metro, by bus and coach services, as well as by car. The area comprising the airport is surrounded by a crossroad of heavy traffic roads, including Viale Forlanini, a six-lanes road crossing the eastern part of the city and the near ring road extending for 3 km. For this reason, the whole area including the medium-sized airport and the nearby roads can be considered a large source of atmospheric pollutants in Milan.

Figure 2.3.2. *Milano Linate airport position with respect to the city center of Milan.*

2.3.3 Methodology

Scope and objectives of the pilot study

The CNR-ISAC contribution to the "pollution hot-spots" pilot is focused on understanding the influence of the Milano Linate area on the concentration of pollutants in the urban area. The Milano Linate area can be considered a large emissions source, including both a medium-sized airport and a crossroad of heavy traffic roads, such as Viale Forlanini and the near ring road. The exposure estimates in the Linate hotspot have been studied by using targeted fixed-sites measurements and mobile measurements, possibly to be coupled with modeling, of a number of reference pollutants. The pollutants addressed are: the number concentration and size distribution of UFP, particles' optical properties, mass concentrations of $PM_{2.5}$, PM_{10}, BC, and NO_x.

The concentrations measured in Linate and the concentrations variability are compared with the urban background site of Milano Pascal, which is composed of three different measurement sites located within the same area (200 m). Moreover, an exercise of Urban Air Quality mapping was planned by using both targeted and opportunistic measurements with volunteer citizens/workers. In particular, we planned mobile measurements by installing an ad hoc developed instrumented box to be placed on an electric bus (73 bus line, from city center to Linate airport) and by installing mobile compact aethalometers on delivering-goods bikers during specific campaigns.

Indeed, this study is taking advantage of using both the traditional observation strategy, based on fixed measurement stations together with some more innovative mobile measurements in a complementary approach for fine scale mapping and the evaluation of hot spots emissions.

Indeed, urban background concentrations of particulate pollutants are pivotal for characterizing the base state of air quality within urban environments, providing a broad overview of the inhabitants' average exposure. Nevertheless, their actual exposure is contingent upon individual daily behavioral patterns and durations spent

RI-URBANS (http://www.RIURBANS.eu) is supported by the European Commission under the Horizon 2020 – Research and Innovation Framework Programme, H2020-GD-2020, Grant Agreement number: 101036245

indoor versus outdoor environments. Additionally, since aerosol particles are a short-lived species their level concentrations exhibit considerable variability over short distances, peaking proximate to emission sources such as traffic hubs and inadequately ventilated settings. This variability becomes of extreme importance when assessing the genuine exposure of individuals residing, laboring, or traversing through pollution epicenters, and is inadequately captured by urban background concentrations (Dons et al., 2019).

In this context, mobile measurements furnish real-time insights into pollution's spatial heterogeneity that can be contrasted with outputs from air quality models that aim to furnish detailed spatial descriptions. Nonetheless, prevalent literature reveals constraints in spatial and temporal coverage primarily due to resource intensiveness (Peters, 2014; Alas et al., 2020). In the frame of the RI-URBANS project, it is intended to examine the spatial dispersion of BC concentrations and ultrafine particle size distribution and its seasonal fluctuations within one of Europe's most polluted urban agglomerations, Milan.

Observation strategy

The observation strategy was based on three different activities: observations at the hot-spot area, at a reference UB site and the mobile measurements. Figure 2.3.3 shows where the different observation sites were located.

Figure 2.3.3. *Area where the fixed and mobile measurements occurred during the 2023 field campaign were located. The orange line represents the route of line 73 bus (targeted mobile measurements on a planned fixed route), while the blue area represents the area where the opportunist measurements are performed, by using existing delivery cyclists' daily routines.*

RI-URBANS (http://www.RIURBANS.eu) is supported by the European Commission under the Horizon 2020 – Research and Innovation Framework Programme, H2020-GD-2020, Grant Agreement number: 101036245

We chose as a reference site of urban background the area of Milano Pascal, where several measurements of atmospheric pollutants were carried out at the same time. This area is composed by three different sites within 200 m distance: the ARPA Lombardia monitoring station (in Via Pascal, Milan), the CNR-ISAC mobile van located in the CNR area (via Alfonso Corti 12, Milan), and the University of Milan (Physics and Chemistry departments) hosting the measurements carried out by the University of Helsinki. The Milano Pascal area is located in the university area, mainly residential and it is considered to be the urban background station of the city; the average population density is 7500 km−2 in Milan (ISTAT, 2020).

In order to study the variability of pollution sources in the Linate airport area, a mobile van (the AERosol mObile LABoratory - AEROLAB) hosting the instruments was installed in the parking lot of Linate airport. Field measurements were conducted from the 19th of January 2023 to the 21st of September 2023.

Through the collaboration with a local delivery enterprise facilitating courier services via bicycle expedition, we planned four campaigns to monitor BC spatial variability at the microscale. With this strategy, the spatial sampling constraints are overcome and the seasonal sampling allows having a broader temporal description than what is usually reported in literature. So far, we performed two campaigns, one in autumn and one in winter, and we will complete the measurements with two more campaigns in spring and summer 2024.

Concerning the bus measurements, after long interactions with the municipality and the urban public transport agency we ended having a formal agreement between the parties. However, we are still facing some technical issues that need to be solved, especially concerning the power supply management.

The "hot-spot" observation site (AeroLab at Milano Linate)

The AERosol mObile LABoratory (AEROLAB) was designed and implemented by CNR-ISAC in 2016 to perform in-depth field characterization of particulate matter in support and/or in the absence of monitoring stations. AEROLAB operates on board a motorhome van so to be easily transferred to any destination, to be set-up and operative within 2-3 hours, and run h24 in a comfortable working space. The van has temperature and humidity control systems to make it operable in Mediterranean regimes [approx. from -5°C to 40°C].

Since its development, AEROLAB has been equipped with state-of-the-art instrumentation for the in situ optical (scattering and absorption) and physical (nano to micrometric size) characterization of aerosols, plus ancillary meteorological variables. The aerosol sampling line has a PM_{10} head with nafion-dryer and an isokinetic splitter that divides the flow to the different analyzers. In situ measurement of trace gases (NO_2 - NO- NO_x), with a dedicated sampling line, has been added for this campaign. These are the instruments deployed during the AEROLAB field campaign in Milano Linate:

- Scanning Mobility Particle Sizer (TROPS-SMPS): aerosol size distribution 10nm - 800 nm;
- Aerosol Particle Sizer (TSI-APS) / Optical Particle Counter (GRIMM-OPC): aerosol size distribution 5/300nm - 10 µm;
- Aethalometer (Magee-AE-33): absorption coefficient and equivalent BC concentration (7 λ) ;
- Nephelometer (AECOM-Aurora 3000): aerosol scattering and backscattering coefficients at 3 λ;
- meteorological parameters (T, P, RH, WS, WD).

The AEROLAB was located in the airport parking, below the take-off route of main flights (see Figure 2.3.4).

RI-URBANS (http://www.RIURBANS.eu) is supported by the European Commission under the Horizon 2020 – Research and Innovation Framework Programme, H2020-GD-2020, Grant Agreement number: 101036245

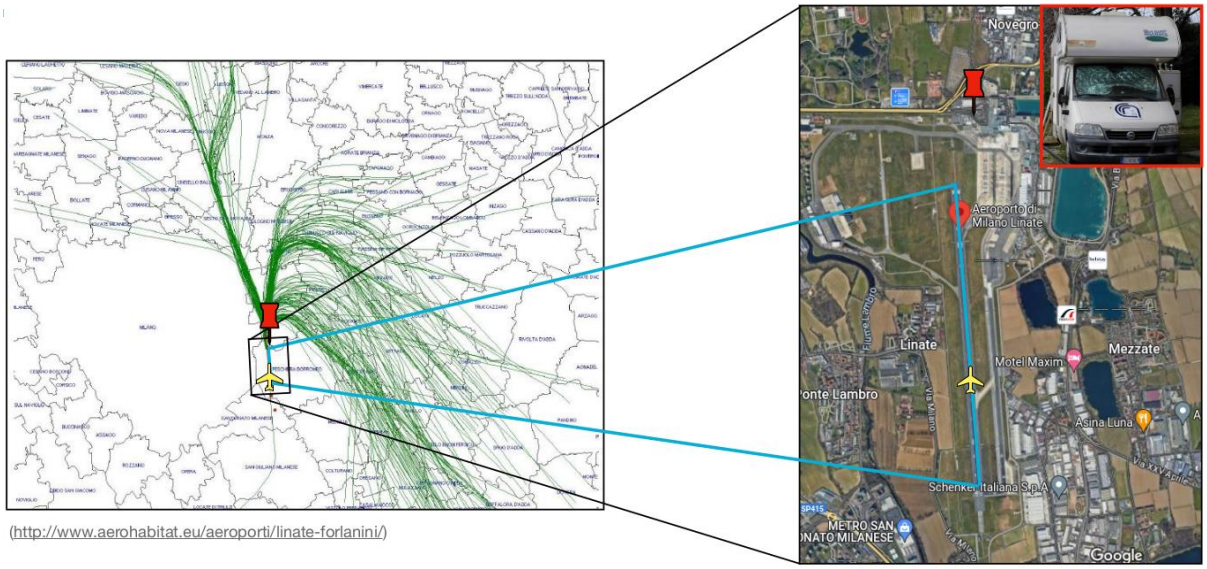

Figure 2.3.4. *Map of Linate airport, location of the AEROLAB and main take-off route of flights.*

During the 2023 field campaign the average number of daily flights ranged between 270 and 350 per month departed/landed from/to the airport of Milano Linate (Figure 2.3.5), while the total number of flights occurred from 19/01/2023 to 31/07/2023 is 59700.

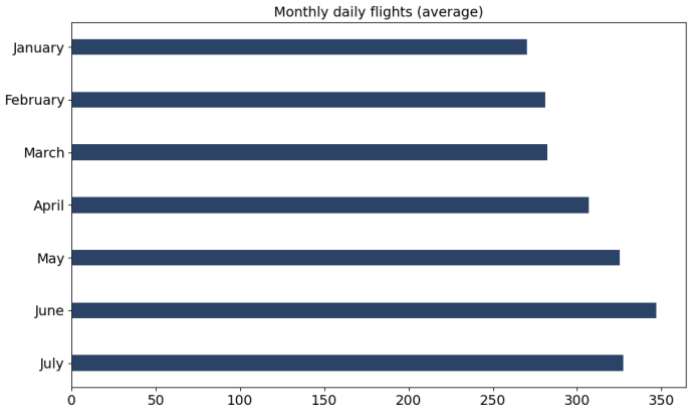

Figure 2.3.5. *Average number of daily flights departed/landed from and to the airport of Milano Linate from 19/01/2023 to 31/07/2023 during the months of the RI-URBANS campaign.*

The background reference site (the area CNR-Milano Pascal-Uni Milan)

The background reference site was located in the University area and it is composed by three sites within 200 m distance:

- Voyager 3 mobile van, a trailer from CNR-ISAC located in the Milano CNR area.
- Milano Pascal ARPA Lombardia (the local environmental agency), in a container carrying out the routine regulated air quality parameters.
- Milano University (Department of Physics and Chemistry), in a laboratory hosting Helsinki University instrument for ultrafine size distribution (SMPS, NAIS, PSM).

RI-URBANS (http://www.RIURBANS.eu) is supported by the European Commission under the Horizon 2020 – Research and Innovation Framework Programme, H2020-GD-2020, Grant Agreement number: 101036245

The CNR-ISAC mobile laboratory, named Voyager3, was located within the research area of the National Research Council (CNR) in Milan (Northern Italy; 45°28’47"N 9°13’54"E; 120 m a.s.l.) (Figure 2.3.6).

Figure 2.3.6. *The Voyager3, a mobile trailer instrumented for aerosol and gas chemistry measurements, located at the CNR area in Milan during the months of the RI-URBANS campaign.*

Specifically, the site is located within the private parking lot of the CNR research area, entirely enclosed by buildings and it's positioned between two heavily trafficked thoroughfares: Viale Abruzzi, the eastbound section of the eastward section of the city's circumferential road and the A51 highway. Notably, the site is located approximately 130 m from the ARPA (Agenzia Regionale per la Protezione Ambientale) Lombardia measurement supersite “Milano Pascal”, categorized as an urban background station according to the criteria used by the EEA, aiming to measure urban background pollution as well. The Voyager3 laboratory, managed by the CNR Institute of Atmospheric Sciences and Climate (ISAC) of Bologna, is equipped with advanced instrumentation for analyzing atmospheric chemistry. During the entire monitoring campaign from late January 2023 to the end of 2023, the Voyager 3 was instrumented with the following measurements:

- ToF-ACSM for the online aerosol chemistry.
- and the Aethalometer AE33 for absorption coefficient and BC concentration.
- VOCUS-PTR-MS 2R for high resolution volatile organic compounds determination.
- Picarro for CO_2, CH_4, H_2O_2 (since July 2023).
- NOx (since September 2023).

Black carbon urban spatial mapping

BC concentrations across the main streets of Milan downtown were monitored by the deployment of a set of micro-Aethalometers (microAeth®, models AE51 and MA200, AethLabs, San Francisco, CA, USA) together with GPS trackers on the bikes of the local courier service: Urban Bike Messengers (UBM). The micro-Aethalometers AE51 and MA200 are portable filter-based absorption photometers that follow the same operational principle as the stationary version described in the previous sections, AE33, except that AE51 reports BC only at 880 nm and does not apply an online correction for loading.

The reason for using different models of micro-Aethalometers emerged from the unexpected malfunctioning of the newer model (MA200) during the autumn campaign. During each seasonal 2-weeks campaign (up to now, during autumn and winter), an area of nearly 25 Km^2 was covered from Monday to Friday between 9:00 and 18:00 local time measuring BC at 30, 10 and 1-second time resolutions, and with average flow rates of 150 ml min^{-1}.

RI-URBANS (http://www.RIURBANS.eu) is supported by the European Commission under the Horizon 2020 – Research and Innovation Framework Programme, H2020-GD-2020, Grant Agreement number: 101036245

To assure the accuracy of the data, pre-, mid- and post- campaign inter-comparisons are performed among the instruments as well as with a reference aethalometer AE33 located in the urban background station in Milan (see Figure 2.3.7 and 2.3.8). The quality control of the data also includes the regular checks of flow and particle free sampling of the devices. Given that the AE51 model does not account for loading artifacts, and a high level of noise is observed in the loading corrected data from the model MA200, an efficient harmonized correction scheme is still being evaluated. Thus, the level concentrations from the portable samplers hereafter presented are the raw data obtained directly from the instruments that will be corrected for loading in the coming reports.

Even though the BC concentrations are tracked with a GPS, the sampling route is based on the delivery routes. Hence, the data needs to be later scrutinized between real sampling periods and stopping periods (in which the measurements can be influenced by local perturbations). The values presented in this report include only the periods in which the samplers were deployed away from the company's headquarters. The discrimination between real sampling and stopping periods remains to be implemented for future reports. Moreover, the geo-position records are taken at an average 30-second time resolution, for which the position of the samplers between to records of positional data were interpolated to match the time resolution of the BC monitors. Finally, the BC concentrations can be paired with their corresponding geolocation, and projected into city maps that can allow the visual identification of pollution hotspots, which will be presented in the following section. However, a method to aggregate the BC concentrations of overlapping geo locations is still under development.

***Figure 2.3.7**. Intercomparing among the micro-aethalometers and the reference instrument AE-33 were carried out before, during and after the bike field campaign.*

***Figure 2.3.8.** A UBM bike ready to start the daily monitoring on Milan roads.*

RI-URBANS (http://www.RIURBANS.eu) is supported by the European Commission under the Horizon 2020 – Research and Innovation Framework Programme, H2020-GD-2020, Grant Agreement number: 101036245

2.3.4 Results and Discussion

Data acquisition and time series analysis

Figure 2.3.9 shows the time series of equivalent BC mass concentration, total particle number concentration and NO2 concentration measured at the hot-spot site (Figures 2.3.9A, C, E) and at the background site (Figures 2.3.9B, D) during the time of the campaign at the hot-spot site (January-September 2023). Generally, higher values of equivalent BC mass concentration and total particle number concentration were measured at the hot-spot site compared with the background site. Higher BC mass concentrations were measured during the first months of the campaign at both the hot-spot and the background site (see also the seasonality variability reported in Figure 2.3.10). Also, a larger total particle number concentration was measured at the hot-spot site during the first months of the campaign (Figure 2.3.9C), while a less clear trend is visible on the same measured variable at the background site (Figure 2.3.9D). Nitrogen dioxide concentration varied up to 50 ppb at the hot-spot site, with larger variability during spring and late summer, compared with the summer months. At this stage, a comparison between the hot-spot and the background sites for NO_2 concentration is not possible due to data of NO_2 concentration from the background site not being available yet.

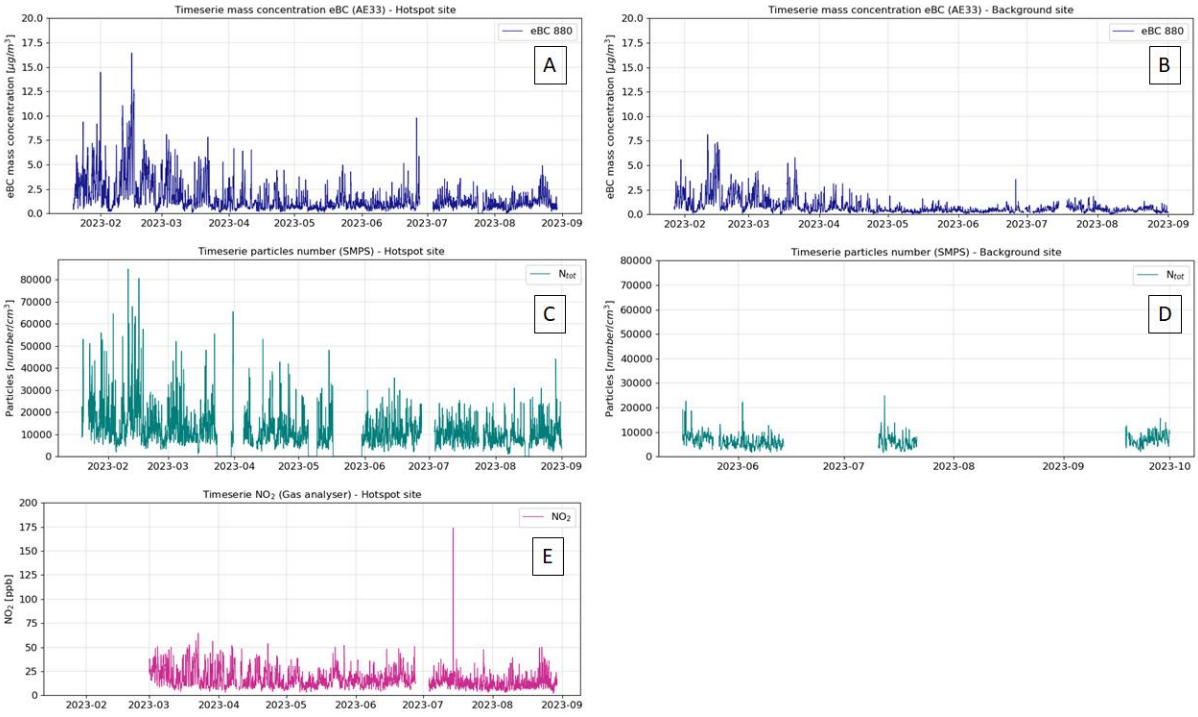

***Figure 2.3.9**. Time series of equivalent BC mass concentration (derived from absorption coefficients measured at 880 nm wavelength) at the hot-spot site (A), the background site (B). Time series of the total particle number concentration measured at the hot-spot site (C) and at the background site (D). Time series of NO_2 concentration measured at the hot-spot site. Data of NO_2 concentration measured at the background site for the same time period are not available yet.*

Comparison between measurements sites and seasonality

Black carbon mean concentrations are compared across the different measurement sites and seasons in Figure 2.3.10. The two reference background sites (here referred as “ARPA” and “CNR”) show no significant differences during the different seasons. As expected, BC concentrations are consistently higher at the hot-spot pollution site than at the background sites. Interestingly, the mobile measurements (“bikes”) show significantly higher BC concentrations in the urban area covered by the measurements than at the hot-spot site and the background sites during wintertime, while comparable concentrations were measured at the urban and hot-spot sites during

RI-URBANS (http://www.RIURBANS.eu) is supported by the European Commission under the Horizon 2020 – Research and Innovation Framework Programme, H2020-GD-2020, Grant Agreement number: 101036245

autumn. The measurements variability represented with the percentiles reported in Figure 2.3.10 is larger at the hot-spot site and in the urban area covered by the mobile measurements, in any season. Black carbon concentration in Milan is larger in wintertime, followed by autumn, spring and summer.

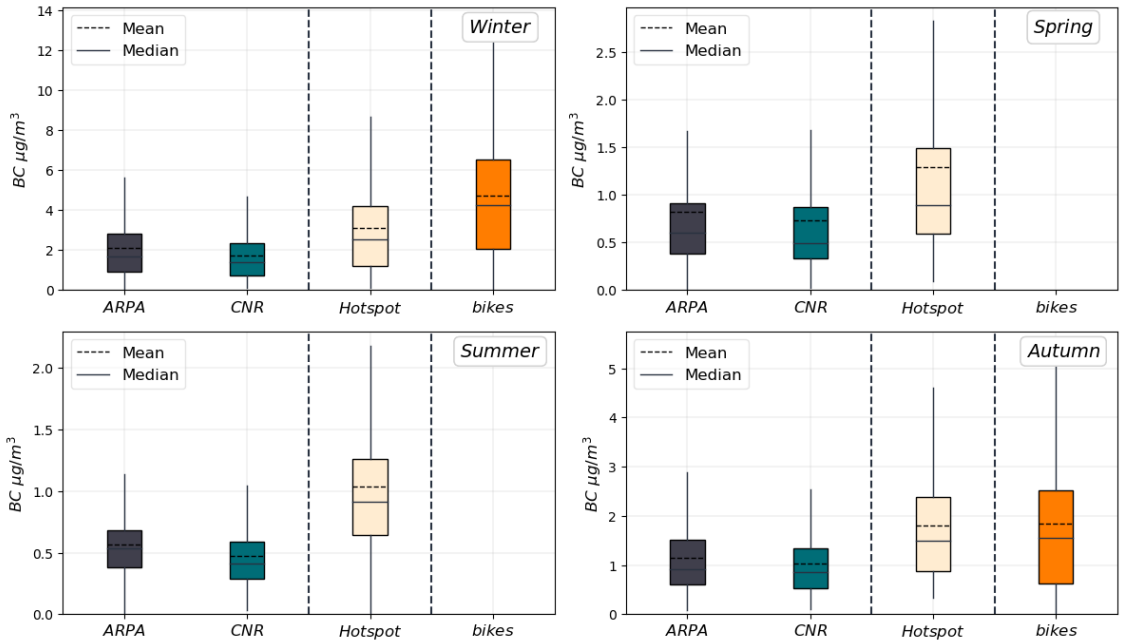

***Figure 2.3.10**. Black carbon mass concentration (derived from absorption coefficients measured at 880 nm wavelength) measured at different sites in Milan (ARPA, CNR= reference background sites, Linate= hot-spot pollution site, bikes= urban area covered with mobile measurements). The box plots represent mean, median values and 25-75 percentiles. Seasonality differences are reported in each panel. Mobile measurements were not available during the spring and summer seasons.*

The total particle number concentration of the ultrafine fraction (Dp < 800 nm) measured during summertime at the hot-spot and the background site is reported in Figure 2.3.11. Significantly higher particle number concentration was measured at the hot-spot site.

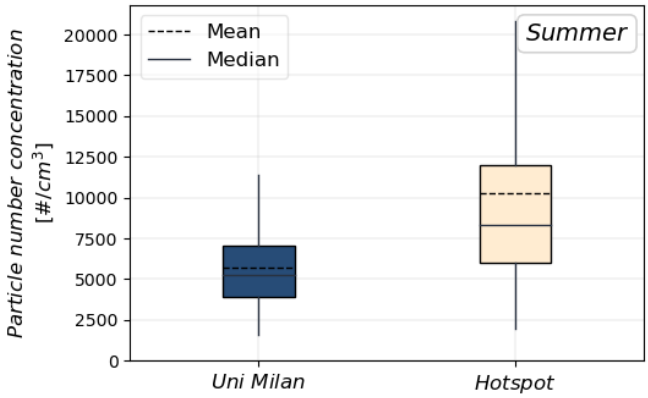

***Figure 2.3.11**. Particle number concentration in the size range 10-800 nm measured with a scanning mobility particle sizer (SMPS, TSI, USA) during summertime in Milan. The hot-spot pollution site is compared with the background site ("Uni Milan"). The box plot shows mean, median and 25-75 percentiles values.*

RI-URBANS (http://www.RIURBANS.eu) is supported by the European Commission under the Horizon 2020 – Research and Innovation Framework Programme, H2020-GD-2020, Grant Agreement number: 101036245

Diurnal variability and source apportionment

The diurnal variability of equivalent BC mass concentration and total particle number concentration during two representative months of the measurement campaign is inspected in Figure 2.3.12 and 2.3.13, respectively.

Source apportionment for the equivalent BC mass concentration was obtained by applying the bilinear model proposed by Sandradewi et al., 2008, considering values of absorption angstrom exponent (alpha) equal to 1.8 for the solid component and alpha equal to 1 for the liquid one, consistent with the values suggested by Zotter et al, 2017.

Figure 2.3.12 shows also the source apportionment of equivalent BC mass concentration, including contributions from solid fuel and liquid fuel consumption. Black carbon concentrations are larger during the night than during the day and peak during the morning and evening hours, corresponding to the rush hours from traffic. The morning and evening peaks are more pronounced at the hot-spot site compared with the background site, and more pronounced in February (chosen for being representative of the wintertime dataset) than July (chosen for being representative of the summertime dataset) (Figure 2.3.12). The contribution from liquid fuel emissions and solid fuel emissions are comparable only during wintertime at the background site, while liquid fuel emissions have a larger contribution than solid fuel emissions during wintertime at the hot-spot site (Figure 2.3.12). Liquid fuel emissions dominate the BC mass concentration at both sites during summertime (Figure 2.3.12). This result agrees with previous studies conducted in Milan indicating the dominant contribution of residential heating to BC emissions during wintertime and the dominant contribution of traffic to BC emissions during summertime (Savadkoohi et al., 2023).

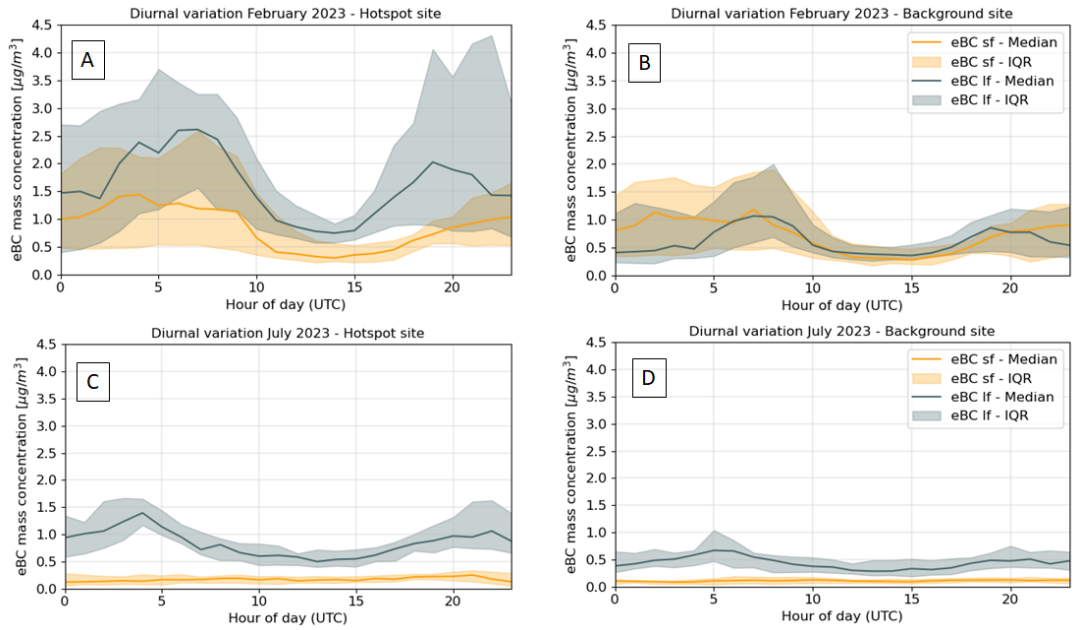

Figure 2.3.12. *Diel profiles of the two main components of median equivalent BC mass concentration at the hot-spot site (A, C), and the background site (B, D), during February 2023 (A, B) and July 2023 (C, D). The shaded areas represent the interquartile range of the measured values. The solid fuel contribution obtained from source apportionment is reported in orange, while the liquid fuel contribution is reported in gray.*

RI-URBANS (http://www.RIURBANS.eu) is supported by the European Commission under the Horizon 2020 – Research and Innovation Framework Programme, H2020-GD-2020, Grant Agreement number: 101036245

Similarly, to BC, the diel profile of the total number particle concentration shows two peaks in the morning and in the evening, more pronounced at the hot-spot site than at the background site, and decreasing concentration during daytime (Figure 2.3.13A, B), likely linked to the vertical atmospheric dynamics. In contrast with the winter months, the total particle concentration measured during summertime at the two sites shows no diel variation (Figure 2.3.13C, D), probably explained by the formation of secondary aerosol, occurring typically during the central hours of the day, when the radiation reaches the maximum. This new particle formation (NPF) increase probably compensates the dynamical dilution that characterizes the other primary variables, such as NO_x and BC.

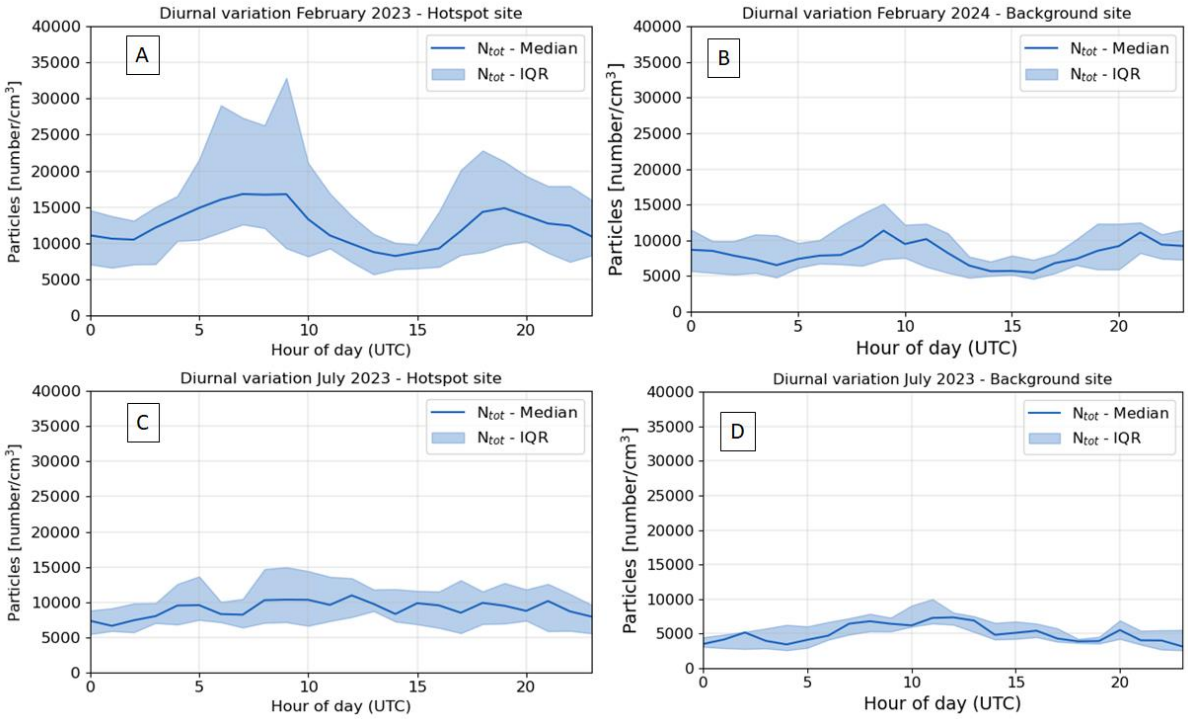

***Figure 2.3.13**. Diel profiles of median total number particle concentration at the hot-spot site (A, C), and the background site (B, D), during February 2023 (A, B) and July 2023 (C, D). The shaded areas represent the interquartile range of the measured values.*

Diel profiles variability with variability boundary layer height

In Figure 2.3.14 and 2.3.15 we investigate the diel variability of BC mass concentration (Figure 2.3.14) and of total particle number concentration (Figure 2.3.15) together with the mixed aerosol layer (MAL) height and the continuous aerosol layer (CAL) height, both representative of the boundary layer height.

It can be seen, in addition to the typical trend, how the diel concentration variability is shaped by the diurnal vertical dynamics, in particular by the MAL dynamics. In fact, the increase in the boundary layer height varies with the decrease of BC concentration and particle number concentration during daytime, pointing at a decrease of these two variables due to a dilution effect. Contrary to our expectations, the month of April presents a rather flat trend for particle number concentration (Figure 2.3.15B).

RI-URBANS (http://www.RIURBANS.eu) is supported by the European Commission under the Horizon 2020 – Research and Innovation Framework Programme, H2020-GD-2020, Grant Agreement number: 101036245

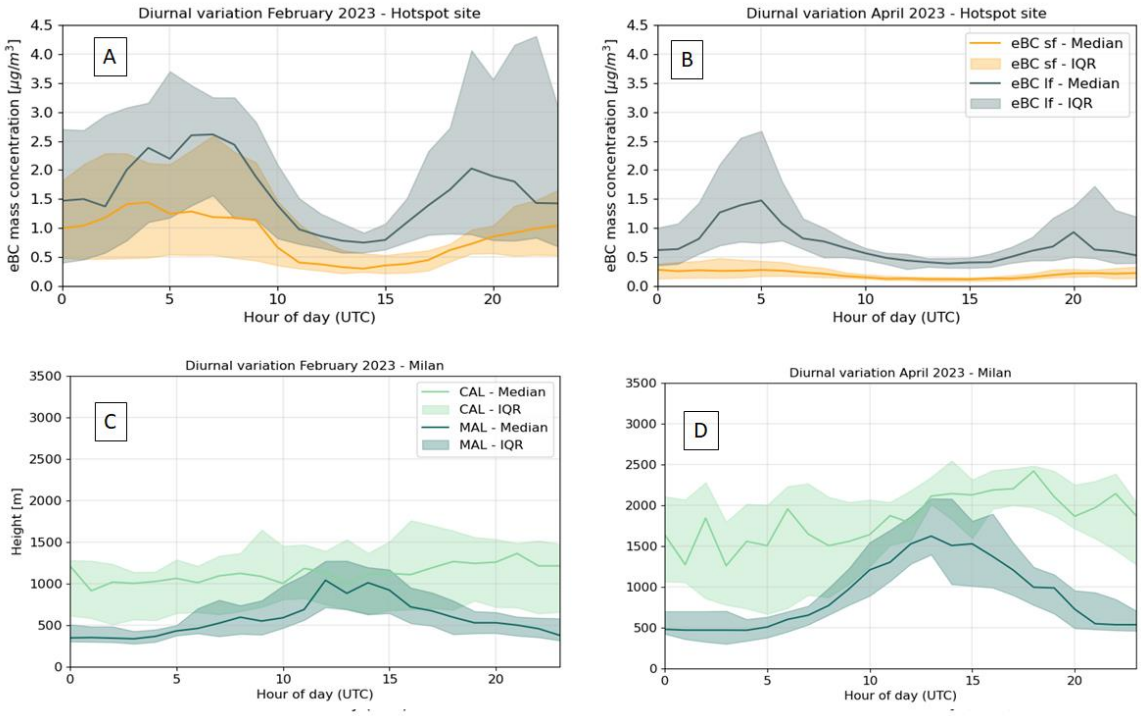

***Figure 2.3.14**. Diel profiles of the two main components of median equivalent BC mass concentration at the hot-spot site during February 2023 (A) and April 2023 (B) and diel profiles of median values of mixed aerosol layer (MAL, in dark green) height and the continuous aerosol layer (CAL, in light green) height at the hot-spot site during February 2023 (C) and April 2023 (D). The solid fuel contribution obtained from source apportionment is reported in orange, while the liquid fuel contribution is reported in gray. The shaded areas represent the interquartile range of the measured values.*

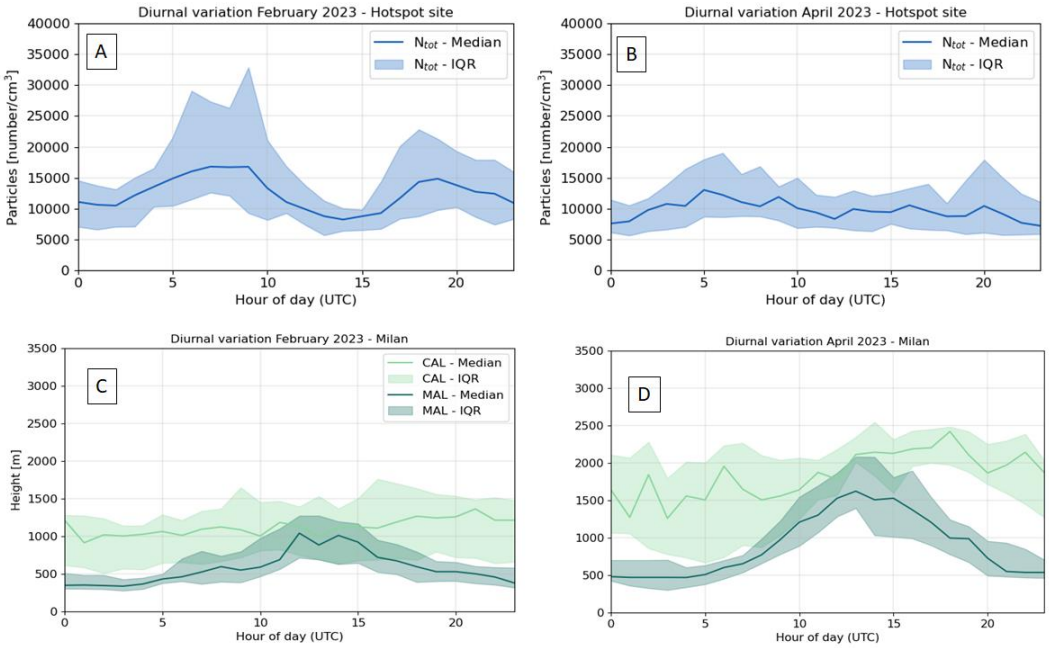

***Figure 2.3.15**. Diel profiles of median total number particle concentration at the hot-spot site during February 2023 (A) and April 2023 (B) and diel profiles of median values of mixed aerosol layer (MAL, in dark green) height and the continuous aerosol layer (CAL, in light green) height at the hot-spot site during February 2023 (C) and April 2023 (D). The shaded areas represent the interquartile range of the measured values.*

RI-URBANS (http://www.RIURBANS.eu) is supported by the European Commission under the Horizon 2020 – Research and Innovation Framework Programme, H2020-GD-2020, Grant Agreement number: 101036245

Impact from flights

A very preliminary analysis was focused to investigate the impact from flights on the number particle size distribution measured at the hot-spot site, and we show here an example of this preliminary work. Figure 2.3.16 shows the number particles size distributions in four consecutive measurements acquired at 08:20, 08:25, 08:30, 08:35 on the 24th of February of 2023 (Figure 2.3.16A) and at 10:10, 10:15, 10:20, 10:25 on the 5th of April of 2023 (Figure 2.3.16B) as examples. The measurements at 08:30 and 10:10 deviate from the typical pattern of the number particle size distributions measured during the same day at different times. Interestingly, the flight number IPRPB occurred at 08:30:30 on the 24th of February of 2023 and similarly the flight number ITY1713 occurred at 10:10:43 on the 5th of April of 2023. We are currently working on the size distribution data to see if flights can explain the observed size distribution patterns.

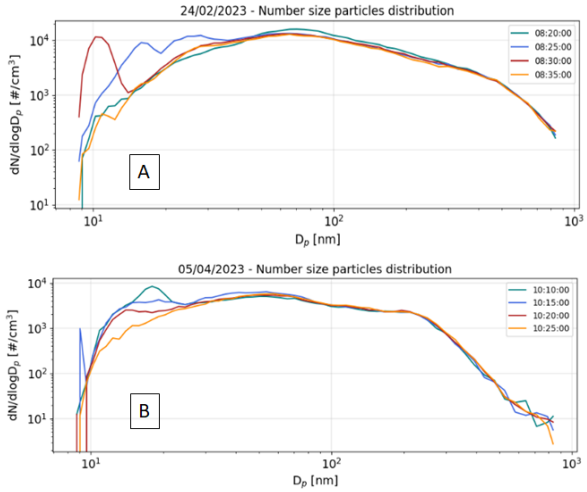

Figure 2.3.16. *Number size distributions measured between 8:20- 10:30 at the hot-spot site during two days, on the 24th of February of 2023 (A) and on the 5th of April of 2023 (B).*

Finally, we show two days of measurements of size distributions at the hot-spot site with contrasting patterns. Clearly, it can be seen that these distributions are strongly disturbed, showing short events (both in spatial and temporal scales) (Figure 2.3.17A) as well as longer nucleation events (pointing at a regional scale event) (Figure 2.3.17B). These two contrasting patterns suggest that the short events are likely caused by local emissions, that can be related both with flights and Viale Forlanini traffic. This point needs a more detailed investigation, that will be carried out once the campaign is ended.

RI-URBANS (http://www.RIURBANS.eu) is supported by the European Commission under the Horizon 2020 – Research and Innovation Framework Programme, H2020-GD-2020, Grant Agreement number: 101036245

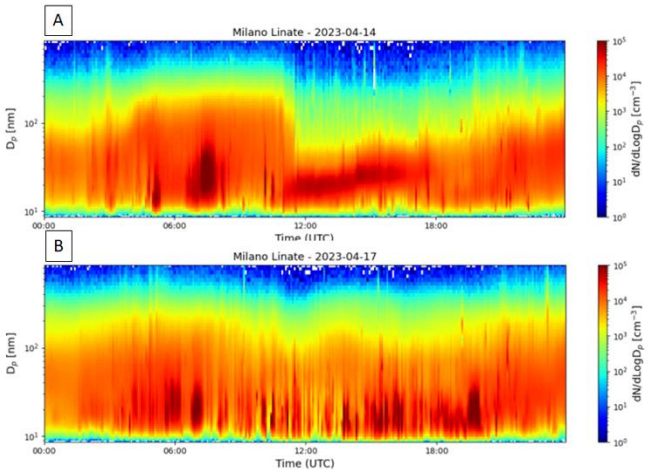

Figure 2.3.17. *Particle size distributions measured at the hot-spot site during the 14th of April 2023 (A) and during the 17th of April 2023 (B).*

Mapping the spatial variability of BC mass concentration

Preliminary results of the autumn and winter campaign show that on road average concentrations were at least 60% higher than the background levels measured at CNR site (background). This difference was observed to increase to 200% during winter (Table 2.3.1).

Table 2.3.1*. Seasonal comparison between mobile and urban background median (IQR) BC concentrations measured simultaneously.*

Season	Urban background BC (mg/m3)	Mobile measurements i BC (mg/m3)
Autumn	1.0 (0.9)	1.6 (1.9)
Winter	2.0 (1.7)	4.3 (4.4)

i Measurements not corrected for loading effect.

Moreover, this difference in median concentrations was also variable throughout the day as can be seen in Figure 2.3.18.

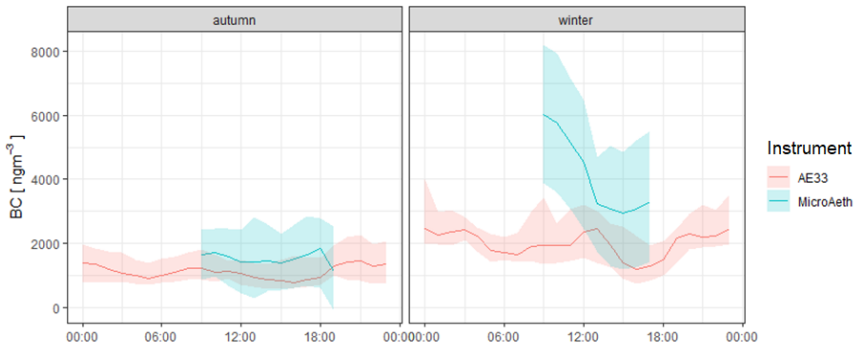

Figure 2.3.18. *Concurrent BC concentrations measured by the mobile samplers and at the urban background station CNR.*

RI-URBANS (http://www.RIURBANS.eu) is supported by the European Commission under the Horizon 2020 – Research and Innovation Framework Programme, H2020-GD-2020, Grant Agreement number: 101036245

The spatial description of the BC mobile measurements is presented in Figure 2.3.19 for autumn and winter campaigns. This figure displays the vast coverage of the sampling. Caution should be made to not overinterpret the hotspots observed at this point since the data still needs to be aggregated spatially to evaluate the statistical representativeness of each data point. Nevertheless, these results emphasize the importance of combining fixed observation points with mobile mapping for a better representation of the exposure of the population in Milan, especially for the people living near or working in traffic sites.

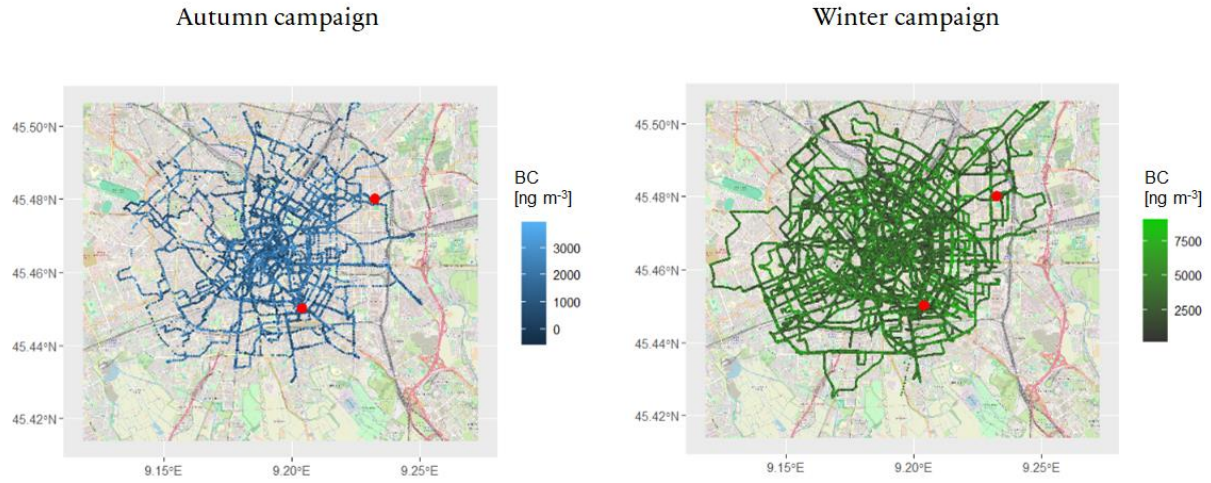

Figure 2.3.19. *Spatial mapping of measured BC concentrations during autumn and winter campaigns. The different color scales represent the concentration ranges observed in each campaign. The red circles mark the location of the CNR station and the UBM headquarter, the starting point of the sampling routes.*

2.3.5 Conclusions and future work

Our preliminary analysis on the data acquired (equivalent BC mass concentration, particle number concentration, particle size distribution and NO_2 concentration) at the hot-spot site (international city airport of Milano Linate) and at the background reference site (Milan University area) shows consistently higher BC mass concentration and total particle number concentration measured at the hot-spot site than at the background site. Higher concentrations were observed during wintertime than summertime, in line with previous measurements conducted in Milan and other urban sites in Europe. The source apportionment on the equivalent BC mass concentration revealed that residential heating and traffic contributed equally during wintertime at the background site, while fossil fuel combustion is the dominant source at the hot-spot site during winter and during summer, as well as the dominant source at the background site during summer. This finding confirms what previous source apportionment studies at urban and background-urban sites in Milan reported. Additionally, our findings indicate that Linate airport is both a concentration hot-spot and a traffic hot-spot in any season. The diel variability of equivalent BC mass concentration and particle number concentration is largely explained by the traffic rush hour peaks in the mornings and evenings, and the atmospheric dilution effect due to the increase in the boundary layer height during daytime. We reported here the preliminary results of the BC mass concentration spatial distribution in the city of Milan obtained from a bike campaign conducted during two seasons. Interestingly, the urban area tracked with the bike campaign showed higher BC concentrations than the background site and the hot-spot site during wintertime, and comparable concentrations with the hot-spot site during autumn. Our future work consists in completing the data analysis on the pollutant NO_2 and ultrafine particle size distribution in order to have a complete overview of the data measured at the hot-spot site. We will compare the size distribution of the two sites, studying the influence of high emissions on the NPF events and secondary aerosol production. We would like to evaluate the impact from

RI-URBANS (http://www.RIURBANS.eu) is supported by the European Commission under the Horizon 2020 – Research and Innovation Framework Programme, H2020-GD-2020, Grant Agreement number: 101036245

flight emissions on all the measured pollutants, especially in term of particle size, optical properties and NO2 concentration, how the flight emission source contributes to the measured values compared to the other pollution sources from the city of Milan. Finally, we would like to use the observed temporal and spatial variability of BC mass concentration to see how this is dispersed in the city and in the metropolitan area of Milan with a model currently under development at another RI-URBANS partner institution (PSI).

2.3.6 References

https://milano.repubblica.it/cronaca/2023/04/23/news/milano_mappa_piste_ciclabili-397389058/, accessed on 12/03/2024

https://www.infodata.ilsole24ore.com/2020/02/14/ogni-dieci-milanesi-quasi-nove-veicoli-circolanti-quante-auto-ci-sono-in-lombradia/, accessed on 12/03/2024

G.M Marcazzan, M Ceriani, G Valli, R Vecchi, Source apportionment of PM10 and PM2.5 in Milan (Italy) using receptor modelling, Science of The Total Environment, Volume 317, Issues 1–3, 2003, https://doi.org/10.1016/S0048-9697(03)00368-1.

K.R. Daellenbach, M. Manousakas, J. Jiang, T. Cui, Y. Chen, I. El Haddad, P. Fermo, C. Colombi, A.S.H. Prévôt, Organic aerosol sources in the Milan metropolitan area – Receptor modelling based on field observations and air quality modelling, Atmospheric Environment, 307, 2023, https://doi.org/10.1016/j.atmosenv.2023.119799.

Jisca Sandradewi, Andre S. H. Prévôt, Sönke Szidat, Nolwenn Perron, M. Rami Alfarra, Valentin A. Lanz, Ernest Weingartner, and Urs Baltensperger, Environmental Science & Technology 2008 *42* (9), 3316-3323, DOI: 10.1021/es702253m

Savadkoohi, M., Pandolfi, M., Reche, C., Niemi, J.V., Mooibroek, D., Titos, G., Green, D. C., Tremper, A.H., Hueglin, C., Liakakou, E., Mihalopoulos, N., Stavroulau, I., Artinano, ˜ B., Coz, E., Alados-Arboledas, L., Beddows, D., Riffault, V., De Brito, J.F., Bastian, S., Baudic, A., Colombi, C., Constabile, F., Chazeau, B., Marchand, N., Gomez-Amo, ´ J.L., Estell´es, V., Matos, V., van der Gaag, E., Gille, G., Luoma, K., Manninen, H.E., Norman, M., Silvergren, S., Petit, J.-E., Putaud, J.-P., Rattigan, O.V., Timonen, H., Tuch, T., Merkel, M., Weinhold, K., Vratolis, S., Vasilescu, J., Favez, O., Harrison, R.M., Laj, P., Wiedensohler, A., Hopke, P.K., Pet¨ aj¨ a, T., Alastuey, A., Querol, X., 2023. The variability of mass concentrations and source apportionment analysis of equivalent black carbon across urban Europe. Environ. Int. 178, 108081 https://doi.org/10.1016/j.envint.2023.108081

Dons, E., Laeremans, M., Orjuela, J. P., Avila-Palencia, I., de Nazelle, A., Nieuwenhuijsen, M., Van Poppel, M., Carrasco-Turigas, G., Standaer, A., De Boever, P., Nawrot, T. & Panis, L. I. (2019). Transport most likely to cause air pollution peak exposures in everyday life: Evidence from over 2000 days of personal monitoring. *Atmospheric environment*, *213*, 424-432.

Alas, H. D. C., Müller, T., Weinhold, K., Pfeifer, S., Glojek, K., Gregorič, A., Močnik, G., Drinovec, L., Costabile, F., Ristorini, M., & Wiedensohler, A. (2020). Performance of microAethalometers: Real-world Field Intercomparisons from Multiple Mobile Measurement Campaigns in Different Atmospheric Environments. *Aerosol and Air Quality Research*, *20*(12), 2640–2653. https://doi.org/10.4209/aaqr.2020.03.0113

Peters, J., Van den Bossche, J., Reggente, M., Van Poppel, M., De Baets, B., & Theunis, J. (2014). Cyclist exposure to UFP and BC on urban routes in Antwerp, Belgium. *Atmospheric Environment*, *92*, 31–43. https://doi.org/10.1016/j.atmosenv.2014.03.039

Sandradewi J, A.S.H. Prévôt, E. Weingartner, R. Schmidhauser, M. Gysel, U. Baltensperger. A study of wood burning and traffic aerosols in an Alpine valley using a multi-wavelength Aethalometer, Atmospheric Environment, 42 (1) 101-112, (2008) https://doi.org/10.1016/j.atmosenv.2007.09.034.

RI-URBANS (http://www.RIURBANS.eu) is supported by the European Commission under the Horizon 2020 – Research and Innovation Framework Programme, H2020-GD-2020, Grant Agreement number: 101036245

3. Summary and Conclusions

Preliminary and intermediate results were shown of the hot spot campaigns conducted in Rotterdam (NL), Bucharest (RO) and Milano (IT). Further analysis and modelling efforts are ongoing.

The approaches between the cities were different. This means that after the final analysis of the individual experiments, a phase of integration will be done in order to 'upscale' the approach and lessons learned can be taken along to be implemented in other urban areas and metropoles.

RI-URBANS (http://www.RIURBANS.eu) is supported by the European Commission under the Horizon 2020 – Research and Innovation Framework Programme, H2020-GD-2020, Grant Agreement number: 101036245